Reviewing of the paper NPG80-2014-80

I performed a review with new eyes and I decide to change a few things in the paper.

I changed the title, I added the word equilibrium before temperature, and so the new title "Equilibrium temperature and Hadley cell in an axisymmetric model" explains better the paper.

I removed the discussion about the old figure 4, it did not address really the problem I wanted to discuss and in my opinion it was misleading in some respects. I also removed the former fig. 11. I changed also the representation of present figures 5, 8 and 11 (former 6, 9 and 13)

There were too much "temperature" words where I meant "equilibrium temperature", although the temperature tries to adjust to the equilibrium temperature, rarely they coincide. I changed in according with I meant (I hope that all be coherent, now).

I addressed almost all the referees' observations. My replies are in the following pages.

==
Reply to referee #1

I would like to thank the referee 1 for his doubts and for his corrections. I want to thank him even for making clearer the paper. I made his doubts mine and I will answer all questions, however in a very few points I cannot understand the referee.

This paper takes an idealized approach to understanding the relationship between the atmospheric circulation and the atmosphere's thermal structure. The model is axisymmetric and there are parameters that allow for varying both the meridional and vertical structure of the equilibrium temperature profile. The experimental design is different from earlier studies in that the equator-pole temperature contrast is held fixed throughout, but the global mean temperature is allowed to vary as the thermal profile is changed.

Overall, the approach taken in this paper is an interesting one, but I have serious reservations about the physical basis for using this model. I understand that the model is idealized, but there should be some way of connecting phenomena in an idealized model to the real atmosphere, and in my view, this paper does not succeed in doing
this. One problem is that the "jets" in this model appear to be driven by completely different physics than the jets in other models, or the jets in the real atmosphere. In more realistic models, the subtropical jets would form near the poleward edge of the Hadley Cell (HC), reflecting a strong contribution from angular momentum conservation. And the midlatitude jet would be located beyond the HC edge. In this model the jets sit equatorward of the stream function maximum.

I cannot understand the statement of the referee since it is very clear that the subtropical jets are located near the poleward edge of the Hadley cell and poleward the maximum stream function (cf. Table 1 -pag 1642 and Figure 3a -pag 1645).

So I am not sure what is generating the jet in this model and what it tells us about the midlatitude or subtropical jets in the real atmosphere.

It is not clear to me what the referee means for midlatitude jet since the model is not able to produce midlatitude jets and so I cannot see how it can tell us something about midlatitude jet.

More problematic is the discussion on p.1632 and Fig. 5, which shows that the difference between potential temperature and equilibrium potential temperature $(\theta - \theta_E)$*is not conserved. This model uses a "Newtonian cooling" scheme to mimic radiative processes, and in such a scheme,* $(\theta - \theta_E)$ *is directly proportional to the diabatic heating, which is in turn directly proportional to the vertical velocity (Held and Hou 1980, eq. 9c). So the fact that* $(\theta - \theta_E)$*is not globally conserved implies that the global integral of vertical velocity is non-zero, which implies that mass is not being conserved. Unless there is some way of correcting this, I do not see a physical basis for using this model at all, and I cannot consider this paper acceptable.*

The referee cites Held and Hou 1980, eq. 9C, page 518, but eq. 9C is a linear equation obtained by approximating the thermodynamics equation, but we are working with a full nonlinear version. Thus it is clear that we are in a breakdown situation of that approximation since the model is able to reproduce well the Hadley cells and subtropical jets. The interesting thing, in my opinion, is that the model produces about the same behavior; a HC more or less extended but with subtropical jets at the same position (about 28°) for almost all the

experiments, even with different stratifications. I find also interesting the difference $(\theta - \theta_E)$ when k is different from one (see new Fig. 4).
The parameter k is equivalent to change the vertical stability; Cessi (1998) showed in her analytical solution that stratification plays a role of diffusivity that can be even negative for unstable stratifications. However Cessi's results come from an approximation of the full nonlinear model equations. I suppose that a negative diffusivity is present here when k=0.5 and strong positive diffusivity is present when k=3. This latter case is intuitive enough, k=3 means that horizontal isotherms become closer and closer at upper levels making the atmosphere very stable there, so the upward branch of the HC has to do more work to go in upper levels, and this also the reason the maximum is located at lower levels, whereas it is located at upper levels when k=0.5 (I added a new paragraph, discussing the new Fig. 4, to explain this, the conservation of $(\theta - \theta_E)$, in the classic definition of Held and Hou is obtained for k=1, instead). Thus it appear quite interesting to me to analyze the model results changing k even though the applications to the real world could be questionable.

1623 L9: *"have been" –> "have also been"*

Thank you for the suggestion.

1624 L15, *"horizontal variable" –> "horizontal coordinate"*

Thank you for the correction. It is greatly appreciated.

1627 L20: It is interesting that you choose an approach that allows the global mean temperature to change as you vary n and k, and I think you should justify this a bit more. Chen et al. (2013) showed that for a uniform SST forcing there is Hadley Cell expansion. Of course, uniform SST warming does not necessarily mean that the warming of the atmosphere is uniform. But it does raise the possibility that some of the HC widening is due just to the increase of global mean temperature, rather than changes in the temperature distribution. Your discussion of HL92 on p.1629 seems to hint at this, but you do not address it explicitly

It is largely recognized that what drives the Hadley circulation is mainly the horizontal gradient, however in my opinion the role of the equator-pole temperature gradient is overstressed whereas what that has really importance is the tropical gradient and I kept constant the equator-pole equilibrium temperature gradient, with *n* changing, to demonstrate this. Moreover, as the referee can see the widening of Hadley circulation can be due to an increase of temperature if this changes the temperature gradient at the equator. I hope that the new version of the paper addresses the problem.

1630 L9: "Since the circulation intensity changes greatly in our experiments, it is problematic to define a width of the Hadley cell based on the absolute value of the circulation itself." This is not an issue in the real atmosphere because there is a clear zero line, which is not the case in this axisymmetric model. So this sentence is a bit misleading.

I meant that in the model there is not a clear edge, I changed the sentence.

1630: "The width of the cell will be defined more or less by isolines having 1/4 of the maximum value of the stream function." This is not a precise definition. Was that intentional? "More or less" is sloppy language.

As before, I wanted to define an edge in term of stream function, I could chose ¼, but it is absolutely an arbitrary choice, this is the reason I used more or less. But I think that if it is

clear that the chosen value is arbitrary I would remove more or less.

1630: "Hence in general when n increases, and the total energy input is larger, the stream function is weaker but poleward." You should mention that this is in agreement with Lu et al. (2008), Gastineau et al. (2008), and Tandon et al. (2013).

Thank you for this suggestion.

1631: "Evidently for R = 0.121..." I don't understand this sentence. Please be clearer about how the numerical and theoretical predictions are different.

I removed the part containing this sentence. I did a review myself and I think this part is not clear enough to me too, so it becomes difficult to explain correctly what I really wanted to say.

1633: "Nevertheless the time-dependent solutions never attain..." –> "The instantaneous HC never resembles the symmetric circulation."?

Yes, I meant exactly that the referee wrote.

1633 L20: "by the" –> "when"

Thank you for the correction.

1633 L23: "weaker in " –> "weaker than"?

Thank you for the correction. It is really appreciated

1635: "However, when we use the jet latitude to define the edge of the Hadley cell..." Here, you appear to be treating the jet in your model as analogous to the eddy-driven midlatitude jet, and there is no basis for such a comparison.

I agree completely with the referee, I did not mean the mid-latitude jets, but the subtropical jets are located at the edge of the Hadley cell, so I can define here the edge of the cell by using the location of the subtropical jets. The problem of relating subtropical jets and edge of the Hadley cell in an axisymmetric model can be in somewhat problematic and here, in my opinion, becomes also interesting since when forcing changes the subtropical jet remains at about 28° for most of the experiments. I changed the sentence in order to stress that jet location remains almost constant for almost all the n values.

Fig 4 caption: "Eq. (10)" –> "Eq. (11)

Thank you for the correction. However I removed Fig. 4

==

Reply to referee #2

I would like to thank the referee for his careful reviewer and for all the questions arisen in reviewing the paper.

To my viewpoint this paper is an interesting contribution in the topic and can be published taking into account some minor questions.
1 – In section 2 it is not necessary to explain all the equations, altough some more explanations will be wellcomed. But I have some concerns on the assumptions. Specifically the step between equation 6 and 7 is not clear for me. Figure 1, helps to visualize the physical meaning of n and k. The question is that the election of the experiments between 0.5 and 3 is not well motivated. Why not other interval or other step? This election determines all the subsequent results and therefore must be well motivated under physical assumption.

I wanted to parameterize the change of horizontal and vertical distribution of temperature. Since the parameters used to fit the "present" climate are *n*=2 and *k*=1, it appeared as natural to me to explore the parameters *n* and *k* in the range of 2 and 1 respectively. In my opinion a step of 0.5 was sufficient to explore the space of parameters. I motivated reasons I used the parameterized Eq. 7 from a physical point of view. I changed the organization of the paragraphs close to Eq. 6 and Eq. 7. I added missing information in Figure 1.

The location of maximum zonal wind is somewhat problematic. First of all is always located under 30°, but there is a transition when n=3. To my viewpoint a discussion based on physical constraints would be grateful. What does it means a planet with n=3? Is this a realistic scenario? Perhaps we can see in the next future a situation like
that because of climate change.

A climate with *n*=3 would be defined as a equable planet (Farrell, 1990) i.e. a planet with very small temperature gradient, a situation that is realistic since the Earth has already experimented this situation in the Cretaceous and Eocene, even though the equator-pole temperature gradient was different the tropical temperature gradient was flatter than the present one (see Greenwood and Wing reference). I added a brief explanation of what happen in terms of physics as suggested by the reviewer. Also other values of *n* and *k* can have a physical meaning. I addressed this meaning.

List of relevant changes

Section 2. I added the justification for Eq. 7, I also moved the paragraphs after Eq. 7 before of Eq. 7.

Section 3. I removed the part that described the former Fig. 4. I modify the former Fig. 5 (now Fig. 4) to show the differences $(\theta - \theta_E)$ after the model reaches the equilibrium for a few simulations. I added a discussion for this Figure. I added a discussion on the impact of the different stratifications.

I added an explanation of the abrupt change of the wind speed observed for broad equilibrium temperature distribution.

~~Temperature~~Equilibrium temperature distribution and Hadley circulation in an axisymmetric model.

Nazario Tartaglione

{School of Science and Technology, University of Camerino, Camerino, Italy}

Correspondence to: N. Tartaglione (nazario.tartaglione@unicam.it)

Abstract

The impact of the equilibrium temperature distribution, θ_E, on the Hadley circulation simulated by an axisymmetric model is studied. The ~~temperature~~θ_E distributions that drive the model are modulated here by two parameters, *n* and *k*, the former controlling the horizontal broadness and the latter ~~defining change in~~controlling the vertical ~~lapse rate.~~stratification of θ_E. In the present study, ~~the changes~~variations of the ~~temperature~~θ_E distribution mimic changes of the energy input of the atmospheric system leaving as an almost invariant the equator-poles θ_E difference. Both equinoctial and time-dependent Hadley circulations are simulated and results compared. The results give evidence that concentrated ~~temperature~~θ_E distributions enhance the meridional circulation and jet wind speed intensities even with a lower energy input. The meridional circulation and the subtropical jet stream widths are controlled by the broadness of horizontal ~~temperature~~θ_E rather than the vertical ~~lapse rate~~ ~~k~~stratification, which is important only when ~~the temperature~~θ_E distribution is concentrated at

Definizione stile: Normale: Tipo di carattere: (Predefinito) Calibri, Non sillabare, Non regolare lo spazio tra testo asiatico e caratteri numerici, Allineamento carattere: Linea di base

Definizione stile: Titolo 1: Non regolare lo spazio tra testo asiatico e caratteri numerici, Allineamento carattere: Linea di base

Definizione stile: Titolo 2: Non regolare lo spazio tra testo asiatico e caratteri numerici, Allineamento carattere: Linea di base

Definizione stile: Titolo 3: Non regolare lo spazio tra testo asiatico e caratteri numerici, Allineamento carattere: Linea di base

Definizione stile: Titolo 4: Non regolare lo spazio tra testo asiatico e caratteri numerici, Allineamento carattere: Linea di base

Definizione stile ... [24]

Definizione stile ... [23]

Definizione stile ... [22]

Definizione stile ... [21]

Definizione stile ... [20]

Definizione stile ... [19]

Definizione stile ... [18]

Definizione stile ... [17]

Definizione stile ... [16]

Definizione stile ... [15]

Definizione stile ... [14]

Definizione stile ... [13]

Definizione stile ... [12]

Definizione stile ... [11]

Definizione stile ... [10]

Definizione stile ... [9]

Definizione stile ... [8]

Definizione stile ... [7]

Definizione stile ... [6]

Definizione stile ... [5]

Definizione stile ... [4]

Definizione stile: Testo segnaposto

Definizione stile: Rimando commento

Definizione stile ... [3]

Definizione stile ... [2]

Definizione stile ... [1]

Formattato: Inglese (Stati Uniti)

Formattato ... [25]

the equator. The jet stream position does not show any dependence with n and k, except when the ~~temperature~~θ_E distribution is very wide (n=3) and in such a case the jet is located at the mid-~~latitude~~latitudes and the model temperature clamps to forcing θ_E. Using n=2 and k=1 we have the formulation of the potential temperature adopted in classical literature. A comparison with other works is performed and our results show that the model running in different configurations (equinoctial, solstitial and time- dependent) yields results similar to one another.

1 Introduction

Formattato: Struttura + Livello:1 + Stile numerazione: 1, 2, 3, … + Comincia da:1 + Allineamento: A sinistra + Allinea a: 0 cm + Imposta un rientro di: 0,76 cm

The earth’s atmosphere is driven by differential heating of the earth’s surface. At the equator, where the heating is larger than that at other latitudes, air rises and diverges poleward in the upper troposphere, descending more or less at 30° latitude~~ (subtropics).~~. This meridional circulation is known as Hadley cell. ~~Because of the earth’s rotation, this circulation produces two~~Two subtropical jets at the poleward edges of the Hadley form because of earth rotation and the conservation of the angular momentum. A poleward shift (Fu and Lin, 2011) and an enhanced wind speed of these jets (Strong and Davis, 2007) are associated with a possible Hadley cell widening and strengthening, which has been observed in the last decades (Fu et al., 2006; Hu and Fu, 2007; Seidel et al., 2008; Johanson and Fu, 2009; Nguyen et al., 2013).

There are a few studies suggesting possible causes of these phenomena. One of the theories postulates global warming as a possible cause of Hadley cell widening (Lu et al., 2009). However, the atmosphere is a complex system containing many subsystems interacting with one another and the global warming might not be the only cause that is suggested to explain the widening. Ozone depletion (Lu et al., 2009; Polvani et al., 2011), SST warming (Chen et al., 2013; Staten et al., 2011) and aerosol (Allen et al., 2012) have also been invoked to explain the Hadley cell widening.

Climate models vary to some extent in their response and the relationship between global warming and Hadley cell is not straightforward. For instance, Lu et al. (2007) found a smaller widening than the observed one. Gitelman et al. (1997) showed that the meridional temperature gradient decreases with increasing global mean temperature and the same result can be found in recent modeling studies (Schaller et al., 2013).

Much of our understanding on the Hadley cell comes from theories using simple models (Schneider 1977, Schneider and Lindzen 1977 and Held and Hou 1980, hereafter HH80) and such a simple model will be adopted here in order to understand how temperature distributions can change the Hadley circulation. How much temperature change impacts the real Hadley circulation is not clear yet, perhaps because of discrepancies between observations, reanalysis (~~Weliser~~Waliser et al., 1999) and climate model outputs, although these differences are becoming less marked because of newer observational datasets or correction of the older ones (Sherwood 2008, Titchner et al., 2008, Santer et al., 2008). Hence, it is critical to understand the possible mechanisms behind the cell expansion starting from a simple model.

The objective of this study is to analyze the sensitivity of a model of the symmetric circulation to the radiative-convective equilibrium temperature distribution. Our point of departure is the symmetric model used by Cessi (1998), which is a bidimensional model considering atmosphere as a thin spherical shell. This model will be briefly described in Sect. 2. The model describes mainly a tropical atmosphere, hence it does not allow for eddies. Although eddies may play a central role in controlling the strength and width of the Hadley cell (e.g. Kim and Lee, 2001; Walker and Schneider, 2006), a symmetric circulation, driven by latitudinal differential heating, can exist even without eddies and it is a robust feature of the atmospheric system (Dima and Wallace, 2003). The temperature distributions used in this study represent some paradigms of tropical atmospheres. Among the possible causes that can change temperature distributions there are El Niño, global warming and change of solar activity. We will show, in Sect. 3, that the energy input is not as important as the ~~temperature~~forcing distribution. Our results are consistent with those obtained both by Hou and Lindzen (1992) (hereafter HL92), and recently by Tandon et al. (2013) who performed experiments similar to those described here. The conclusions will be drawn in Sect. 4.

2 The model

Formattato: Struttura + Livello:1 + Stile numerazione: 1, 2, 3, … + Comincia da:1 + Allineamento: A sinistra + Allinea a: 0 cm + Imposta un rientro di: 0,76 cm

The model used in this study is a bidimensional model of the axis-symmetric atmospheric circulation described in Cessi (1998). The horizontal ~~variable~~coordinate is defined as $y = a sin\phi$ from which we have

$$c(y) = cos\phi = \sqrt{(1 - y^2/a^2)} \qquad (1)$$

where a is the radius of a planet having a rotation rate Ω, the height of atmosphere is prescribed to be H.

The model is similar to the Held and Hou model (HH80), but ~~the difference is that, the model~~it prescribes a horizontal diffusion $\nu_H$other than the vertical diffusion ~~-~~ν_v. The prognostic variables are the angular momentum M, defined as $M = \Omega a c^2 + uc$ where u represents the zonal velocity; the zonal vorticity ψ_{zz} with the meridional stream function ψ defined by

$$\cancel{\partial_y\psi \equiv w;}\ \partial_y\psi \equiv w;$$
$$\cancel{\partial_z\psi \equiv -cv}\partial_z\psi \equiv -cv$$

(2)

and the potential temperature θ that is forced towards a radiative-convective equilibrium temperature θ_E. Starting from the dimensional equations of the angular momentum, zonal vorticity and potential temperature, we will obtain a set of dimensionless equations. The new equations are non-dimensionalized using a scaling that follows Schneider and Lindzen (1977), but the zonal velocity u is scaled with Ωa. A detailed description can be found in Cessi (1998).

The non-dimensional model equations are:

$$M_t = \frac{1}{R}\left\{M_{zz} + \mu\left[c^4(c^{-2}M)_y\right]_y\right\} - J(\psi, M) \tag{3a}$$

$$\psi_{zzt} = \frac{1}{(R^2E^2)} yc^{-2}(M^2)_z - \frac{1}{c^{-2}} J(\psi, c^{-2}\psi_{zz}) + \frac{1}{(RE^2c^{-2})}\theta_y + \frac{1}{(Rc^{-2})}\left[c^{-2}\psi_{zzzz} + \mu\psi_{zzyy}\right] \tag{3b}$$

$$\theta_t = \frac{1}{R}\left\{\theta_{zz} + \mu\left[c^2\theta_y\right]_y + \alpha[\theta_E(y,z) - \theta]\right\} - J(\psi, \theta) \tag{3c}$$

The term $J(A,B) = A_yB_z - A_zB_y$ is the Jacobian.

The thermal Rossby number *R*; the Ekman number *E*, the ratio of the horizontal to the vertical viscosity *μ* and the parameter *α* are defined as

$$R \equiv gH\,\Delta_H/(\Omega^2a^2)\,;\;\; E \equiv \nu_V/(\Omega H^2)\,;\;\; \mu \equiv (H^2/a^2)\cancel{\nu_H/\nu_V}\;\; \nu_H/\nu_V\,; \alpha \equiv H^2/(\tau\nu_V) \tag{4}$$

The term α is the ratio of the viscous timescale across the depth of the model atmosphere to the relaxation time τ toward the radiative-convective equilibrium.

The boundary conditions for the set of Eq. 3 are:

$$\begin{aligned} &M_z = \gamma(M - c^2),\;\; \psi_{zz} = \gamma\psi_z\,; \\ &\psi = \theta_z = 0\; at\; z = 0; \\ &M_z = \psi_{zz} = \psi = \theta_z = 0\; at\; z = 1. \end{aligned} \tag{5}$$

Where $\gamma = \frac{CH}{\nu_V}$ is the ratio of the spin-down time due to the drag to the viscous timescale, the bottom drag relaxes the angular momentum *M* to the local planetary value Ωac^2 through a drag coefficient *C*.

The model flow started from an isothermal state at rest and is maintained by a Newton heating function where the heating rate is proportional to the difference between the model potential temperature and a specified radiative-convective equilibrium temperature distribution, which follows the HH80 one:

$$\theta_E = \frac{4}{3} - y^2 + \frac{\Delta_V}{\Delta_H}\left(z - \frac{1}{2}\right). \qquad (6)$$

~~We will assume that Eq. 6 is the radiative-convective equilibrium temperature distribution of the control experiment; we define a general form of the Eq. 6 as~~

Equation 6 is used extensively in dry axisymmetric models (e.g. HH80, Farrell, 1990, Cessi 1998) and it is related to the thermal forcing term of the equation system. A statically stable state as a vertical profile of θ_E is also assumed by Eq. 6. HH80 suggested that the impact of latent heat released by water vapor condensation can be incorporated in dry axisymmetric models by modifying the meridional distribution of θ_E. HL92 followed the HH80 argument and altered the concentration of θ_E under the constraint of equal energy input. The resulting θ_E distributions used by HL92 were peaked distributions on and off the equator resulting in a stronger Hadley circulation with respect the circulation obtained applying Eq. 6.$\cancel{\theta_E = \frac{4}{3} - |y|^n + \frac{\Delta_V}{\Delta_H}\left(z^k - \frac{1}{2}\right).}$ ~~(7)~~

Tandon et al. (2013) used narrow and wide thermal forcing to mimic El Niño or global warming effect on a tropical circulation in a Global Circulation Model.~~The values n and k control the horizontal homogenization of the temperature and the lapse rate respectively.~~ On the opposite side, in fact, we can suppose that if a warmer climate happens, especially in the tropical regions, a very weak gradient of the equilibrium temperature θ_E will be more extent in latitude, expanding consequently the tropical region. This is already occurred in the past, especially in the mid Cretaceous and Eocene when the tropics extended up to 60°. This is the so called equable climate (e.g. Greenwood and Wing, 1995) where roughly equal temperatures are present throughout the world. During those geological ages the temperature was generally higher everywhere, but adding a constant to the temperature does not change the response of this kind of models. The equator-pole temperature gradient was smaller than the present situation, whereas we prescribe constant surface equator-pole θ_E gradient. As we shall show afterwards this is necessary to demonstrate that it is the tropical temperature gradient drives the Hadley circulation. Thus, in order to study systematically these different conditions we adopt the strategy to build forcing functions dependent on a parameter that controls the θ_E gradient in the tropical regions. Since, with different horizontal distributions of θ_E we can figure out that even the vertical distribution could be affected by some physical mechanisms that make the atmosphere more or less stable than the stratification described by the z component of Eq. 6. The meridional and vertical changes of equilibrium temperature can be obtained by changing the exponents of y and z in Eq. 6 transforming Eq. 6 in the following equation:

~~When n=2 and k=1 Eq. (7) becomes the reference equilibrium temperature given in Eq. 6. In many other works (e.g. Schneider 1977, HH80, Caballero et al. 2008), the considered atmosphere is essentially dry; however the distribution of temperature of a dry atmosphere can reflect an action of the water vapor condensation (HL92). Tandon et al. (2013) used narrow and wide thermal forcing to mimic El Niño or global warming effect on a tropical circulation in a Global Circulation Model.~~

$$\theta_E = \frac{4}{3} - |y|^n + \frac{\Delta_V}{\Delta_H}\left(z^k - \frac{1}{2}\right). \qquad (7)$$

The values n and k control the horizontal distribution of θ_E and its stratification respectively. Small values of n are associated with concentrated θ_E distributions. Increasing n means increasing broadness of the θ_E distribution. Values of k larger than 1 mean more stable upper levels, vice-versa smaller k values means lower levels are more stable than upper levels. Thus, it comes quite natural to explore the response of Hadley circulation by changing the parameters n and k, which control the distribution of θ_E, in closest ranges of 2 and 1 respectively. Thus n and k will change from 0.5 to 3 with a 0.5 step, in such a way we have a set of 36 simulations. When n=2 and k=1 Eq. (7) becomes the reference equilibrium temperature given in Eq. 6 and the experiments performed with n=2 and k=1 will be considered as the reference experiments.

The average θ_E~~Starting from Eq. 7 a set of experiments were performed changing n and k in such a way to have a set of numerical results. In order to isolate the contribution of the temperature distribution on the solution of Eq. 3, a set of parameters will be used:~~

Formattato: western, Giustificato, Rientro: Prima riga: 0,85 cm, SpazioPrima: 6 pt

Formattato: Inglese (Stati Uniti)

$$\cancel{a = 6.4 \times 10^6\, m \quad \Omega = 2\pi/(8.64 \times 10^4)\ s^{-1}}$$

$$\cancel{\Delta_H = 1/3 \qquad \Delta_V = 1/8}$$

$$\cancel{g = 9.8\, ms^{-2} \qquad C = 0.005\, ms^{-1}}$$

$$\cancel{H = 8 \times 10^3 m \qquad \tau = 20\, days}$$

$$\cancel{\nu_V = 5\, m^2 s^{-1} \qquad \nu_H = 1.86\, m^2 s^{-1} \qquad (8)}$$

~~The parameters in Eq. 8 are the same as those used by Cessi (1998).~~

~~The meridional and vertical gradients are controlled by the parameters n and k, where they vary from 0.5 to 3 with a 0.5 step, in such a way that we have a set of 36 simulations. The average temperature~~ along the latitudes and heights are shown in Fig. 1. Heating functions with n value equal to 0.5 should not be regarded as unreal, but merely as a simple way to represent a specific state of the atmosphere. The same assertion is valid for all other

Formattato: western, Giustificato, Rientro: Prima riga: 0,85 cm, SpazioPrima: 6 pt parameters. As n increases the average temperature increases as well, but the meridional gradient decreases~~. High n values represent situations with a model atmosphere temperature homogenized along the meridional direction (Fig. 1a).~~ in the tropical regions.

With the prescribed ~~temperature~~θ_E as ~~stated in~~specified by Eq. 7, the ~~temperature~~θ_E values at the boundaries and its equator-pole difference temperature remain invariant with respect to n~~ and~~, for a given k value. The ~~mean temperature~~energy input is not constant here, which differs from HL92, which analyzed the influence of concentration heating perturbing the forcing function θ_E *(y,z)* in such a way that ~~its average~~θ_E averaged over the domain remained constant. It is easily visible in Fig. 1b. Higher n values, keeping k invariant, have higher ~~mean temperatures~~averaged θ_E at all levels. The same is true for k, with higher k values, for n constant~~, the mean temperature for~~; θ_E at each level is always higher than that with lower k values. The pole-equator ~~temperature~~θ_E difference at upper and lower vertical boundaries are the same for all the experiments~~, but~~ having the same k, the ~~meridional (~~vertical~~) temperature gradient~~ averaged θ_E changes as a function of k, for n ~~(k).~~constant. Whether global warming makes the ~~earth~~equilibrium temperature distribution narrower or wider is beyond the aim of the paper. One can expect that global warming broadens the temperature distribution, but at the same time it could have an impact above all on the ~~SST~~sea surface temperature (SST) bringing more water in the upper atmosphere which changes the vertical distribution of the temperature in the ~~intertropical convergence zone.~~inter-tropical convergence zone (ITCZ). It is supposed that, in first approximation, oceans force the atmosphere, so we have to allow for the possibility that increasing SST can change the forcing distribution. Increasing uniformly SST might could a poleward expansion as showed by Chen et al. (2013) with an aquaplanet model, but in that case the mechanism was supposed to be related mainly to mid-latitude eddies rather than a tropical forcing. Since other causes can

Formattato: Inglese (Stati Uniti)

Formattato: Tipo di carattere: Corsivo, Pedice

Formattato: Tipo di carattere: Non Corsivo change the temperature distribution of a planet such as changes in the solar activity for instance, we will focus on the temperature distribution regardless of its cause.

~~Although in~~In this model the atmosphere is dry as in many other studies (e.g. Schneider 1977, HH80, Caballero et al. ~~,~~2008), changing the ~~temperature~~θ_E distribution allows for a change in the static stability. Looking at the ~~mean temperature~~average θ_E along the vertical direction, low values of *k* are related to low values of static stability, especially in higher level of the model atmosphere.

The Brunt–Väisälä frequency~~$N^2 = g\frac{\theta_z}{\theta}$,~~ when the atmosphere reaches the equilibrium will be

$$N^2 = \frac{(gk\Delta_V/\Delta_H z^{(k-1)})}{[4/3 - y^n + \Delta_V/\Delta_H(z^k - 1/2)]}. \qquad (\cancel{9}8)$$

It is clear from Eq. ~~9~~8 that the Brunt–Väisälä frequency does not depend on *n* at the poles and equator. On the contrary, it depends on *k*; large values of *k* imply a more stable atmosphere in the upper levels, especially at poles, making the model atmosphere more similar to the real one, simulating in some respects a sort of tropopause. Moreover, this is equivalent to creating a physical sponge layer in the upper levels of the model that will have some effects on the vertical position of stream function maximum.

Starting from Eq. 7 a set of experiments were performed changing *n* and *k* in such a way to have a set of numerical results. In order to isolate the contribution of the θ_E distribution on the solution of Eq. 3, a set of parameters will be used:

$$a = 6.4 \times 10^6\ m \quad \Omega = 2\pi/(8.64 \times 10^4)\ s^{-1}$$

$$\Delta_H = 1/3 \qquad \Delta_V = 1/8$$

Formattato: Inglese (Stati Uniti)

Formattato: Inglese (Stati Uniti)

Formattato: Inglese (Stati Uniti)

Formattato: western, Giustificato, Rientro: Prima riga: 0,85 cm, SpazioDopo: 9,9 pt

Formattato: Inglese (Stati Uniti)

Formattato: western, Giustificato, SpazioPrima: 6 pt

Formattato: Inglese (Stati Uniti)

Formattato: western, Giustificato, Rientro: Prima riga: 0,85 cm, SpazioPrima: 6 pt

Formattato: Inglese (Stati Uniti)

$$g = 9.8\,ms^{-2} \qquad C = 0.005\,ms^{-1}$$

$$H = 8 \times 10^{3} m \qquad \tau = 20\ days$$

$$\nu_V = 5\,m^2 s^{-1} \qquad \nu_H = 1.86\,m^2 s^{-1} \tag{9}$$

The parameters in Eq. 9 are the same as those used by Cessi (1998).

3 Numerical Results

This section is divided into three subsections, the first showing the results of the model applying the equinoctial condition, when the sun is assumed to be over the equator. The solution is steady as already shown for instance in Cessi (1998). The second subsection will show the results of the model having a ~~temperature~~θ_E distribution described by Eq. 7 but moving following a seasonal cycle. The case n=2 and k=1 is discussed in the third subsection in comparison with previous studies.

3.1 Equinoctial ~~conditions~~simulations

The axially symmetric circulation is forced by axially symmetric heating as in HH80 and many others and as prescribed by Eq. (7). The model started from an isothermal state and it was run for 300 days, even though it reached its equilibrium approximately after 100 days, in order to be sure that the model does not have instabilities in the long run. The stream function values obtained when n=2 and k=1, the reference experiment are about the same of that obtained by HH80. We will show the non-dimensional value, but to have the dimensional values we need to multiply by $\nu_V R \varepsilon^{-1} = 484$ $m^2 s^{-1}$.

Formattato: Struttura + Livello:1 + Stile numerazione: 1, 2, 3, … + Comincia da:1 + Allineamento: A sinistra + Allinea a: 0 cm + Imposta un rientro di: 0,76 cm

Formattato: Struttura + Livello:2 + Stile numerazione: 1, 2, 3, … + Comincia da:1 + Allineamento: A sinistra + Allinea a: 0 cm + Imposta un rientro di: 1,02 cm

The absolute value of the maximum stream function intensity at the equilibrium conditions for the 36 experiments is shown in Fig. 2. When n=0.5, with k constant, the circulation is always the strongest. The stream function intensity is inversely proportional to n (Fig. 2a). With n=0.5 the experiment resembles the one described in HL92 where they concentrated the latitudinal extent of heating and this led to a more intense circulation. However, they imposed the forcing function $\theta_E(x, y)$ in such a way that its average over the domain remained the same as in the control experiment, i.e. without changing the energy input. They found that concentration of the heating through a redistribution of heat within the Hadley cell led to a more intense circulation without altering its meridional extent. Instead, here, it is evident from Fig. 1 that the experiment with n=0.5 has an energy input lower than the other cases. Nevertheless, the Hadley circulation is always more intense than the other cases and contrary to higher n value experiments, the circulation is confined close to the equator. Thus the results of HL92 are extended to a more general case with a lower energy input. It is worth ~~noting~~noticing the constraint of an equal pole-equator gradient of mean ~~temperature~~θ_E is assumed here ~~which is different~~differently from HL92 (Fig. 1a).

The dependence on k is not as straightforward as the one on n, instead. The stream function reaches the highest value for n=0.5 and k=3. With a high n values the Hadley cell stream function intensity is lower and the dependence on k loses its importance. In other words, in our model, the symmetric circulation strength is modulated by k only when the equilibrium temperature distribution is concentrated to the equator.

Figure 2b shows the maximum zonal wind speed as function of n and k, it is inversely proportional to n, the dependence on k is not as clear as the one on n and when n=3 it almost vanishes in accordance with the behavior of the maximum stream function. These results are

Formattato: Tipo di carattere: Corsivo in agreement with HL92, who found a stronger zonal wind when the ~~temperature~~forcing was concentrated at the equator.

Some studies define the border of a Hadley cell as that by the zero line of the 500 hPa stream function (e.g. Frierson et al., 2007). ~~Since~~Since in this kind of model the zero stream function is at the poles, it is problematic to define an edge of the Hadley cell based on the zero stream function. Moreover, the circulation intensity changes greatly in our experiments, so it is problematic to define ~~a width~~an edge of the Hadley cell based on ~~the~~an absolute value of the circulation itself.~~ Moreover the stream function goes to zero in the model only at the poles.~~ Hence, we will define the position of the cell equal to the position of the maximum value of stream function, in this way we will study a possible poleward shift of the cell as a function of the two parameters *n* and *k*. The ~~width~~edge of the cell ~~will~~might be defined ~~more or less~~ by values of isolines ~~having 1/4 of~~that are relative with respect to the maximum value, for example 1/4 of the stream function. ~~It is worth noting that~~For the sake of clarity this definition is an operational one and does not ~~resemble~~follow the definition used for example by Dima and ~~Wallance~~Wallace (2003) or Frierson et al. (2007).

The latitude of the maximum stream function value shows a general dependence on *n* and *k*. It increases with *n* and decreases with *k*. However, as shown in Fig. 3a, this dependence is not straightforward or linear, although we have a few exceptions, for instance when $k=n=0.5$. Hence in general when *n* increases, and the total energy input is larger, the stream function is weaker ~~but~~and the Hadley cell moves poleward. This result is in agreement with other model outcomes (Frierson et al, 2007, Lu et al., 2008; Gastineau et al., 2008; and Tandon et al., 2013). The model predicts a weakening of circulation, in contrast with the ~~recent observations where a slight~~ strengthening~~ and~~, together with widening, of the Hadley ~~Circulation~~circulation for the past three decades ~~was~~ observed by Liu et al. (2012) and~~ a~~

~~poleward expansion was also found by~~ Hu and Fu (2007). However, Liu et al. (2012) showed that if the observations start from 1870, the Hadley cell ~~becomes~~has become more narrow and stronger.

Formattato: Tedesco (Germania)

The height of the maximum stream function value is confined for almost all the simulations under 2200 m and the general rule is that when *n* increases, the height of maximum lowers, however a few experiments, those with *k*=0.5 and *n*=0.5, 1 and 1.5, have the maximum value between 4300 and 5600 m exhibiting an increase in the height with *n* (Fig. 3b).

In general, the location of the maximum zonal wind speed does not show any evident relationship with the parameters *n* and *k*. It is always confined between 26° and 29° off the equator; however when *n=3*, there is an abrupt transition to about 48°, independently from the *k* value. In Table 1, we show the latitude of the maximum wind speed when *k=1* for different *n* values.

Formattato: Tedesco (Germania)

~~It is worth calculating the prediction of the cell edge following the HH80 assumptions. HH80 showed that the Hadley cell has a finite width with the edge ending at a specific latitude φ_H and calculated a scaling for this latitude. Starting with the vertically integrated hydrostatic equation and a balanced zonal wind, HH80 obtained a formulation for θ in the limit inviscid:~~

$$\cancel{\bar{\theta}(\phi) = \bar{\theta}(0) - \bar{\theta}_0 \frac{\omega^2 a^2 sin^4(\phi)}{2gH cos^2(\phi)} \qquad (10)}$$

~~Assuming continuity of the potential temperature $\bar{\theta}(\phi_H) = \bar{\theta_E}(\phi_H)$ and conservation of vertically averaged potential temperature $\int_0^{\phi_H} \bar{\theta}\, cos(\phi) d\phi = \int_0^{\phi_H} \bar{\theta_E}\, cos(\phi) d\phi$, they found φ_H as a function of the Rossby number R. The hypothesis of continuity and conservation of~~

~~potential temperature is equivalent to solving those two equations by means of a geometric "equal area" construction.~~

~~For the general case described by Eq. 7, we calculated a similar relationship between φ_H and the Rossby number, assuming the same hypothesis of HH80 described previously.~~

$$\cancel{R = \left[\frac{(n+1)}{2n}\right]\frac{\left[\left(y_H^{\frac{5}{3}}/(1-y)+y_H+1/3y_H^{\frac{3}{3}}-1/2ln((1+y_H)/(1-y_H))\right)\right]}{y_H^{(n+1)}}} \qquad (11)$$

~~The n value goes from 0.5 to 3. Equation 11 should be compared with Eq. 17 of HH80. We represent the solutions of Eq.11 in Fig. 4. Evidently for R=0.121 (that is the Rossby number used here), there is no agreement when n=3 between analytic solution that predicts a smaller φ_H and the numerical one, which differs from all the other solutions that are quite close to one another.~~

~~This behavior could be related to the diffusivity. Figure 5 shows the analytic and numerical vertically averaged potential temperature for n=k=3. It is evident that not only $\bar{\theta}$ is not conserved when n=3 and there is not redistribution of energy, hence the assumption made by HH80 about the continuity and conservation of potential energy and that leads to Eq. 11 never takes place in the numerical model for n=3. However, when the vertical diffusion is very small or k has low values $\bar{\theta}$ approaches to $\bar{\theta}_E$ (not shown) but the jet streams have their maxima at the mid-latitudes.~~

~~Figure 6 shows the stream function and the zonal wind speed for the experiments n=k=0.5 (Fig. 6a) and n=k=3 (Fig. 6b~~The difference between θ_E and θ, once the model reaches the equilibrium, is quite interesting. Figure 4 shows meridional distributions of θ_E and θ for n=3 and k=0.5, 1 and 3. In Fig. 4a, θ_E is under θ, when k=1 we find θ_E is over θ in a region around the equator (Fig. 4b), with θ_E crossing θ at about 47°, finding again the equal area condition suggested by HH80 and that explains approximately the jet location, whereas in Fig.4c, with k=3, we can see how θ_E is over θ. Despite these differences in the distributions of θ_E and θ the model produces with these different k values almost the same solution, in terms of circulation strength and jet location. For other values of n the results are similar, but the differences between θ_E and θ are not so visible.

We can understand these findings in the light of Cessi (1998) results obtained by expanding the variables M, θ and ψ in power series of R. The term R^2 in nonlinear expansion part, the meridional advection depends on the differences between θ_E and θ, on the cube of the meridional temperature gradient, and linearly on the imposed stratification deducing that for unstable stratifications, this term would appear as a negative diffusivity term (Cessi, 1998), whereas it acts as a positive diffusion. This seems to be the case, in our simulation when k=0.5. The thermal energy obtained in the model is larger than the imposed temperature (Fig.4a). Although the stratification imposed by Eq. 7 is stable, i.e. $\frac{\partial \theta_E}{\partial z} > 0$, the second derivative is negative when k=0.5 reducing the stability at upper levels, so this situation can be seen as a way to simulate the effect of the latent heat released by water vapor condensation. When k=3 the air in upper levels is very stable and the flow has to do more work, giving rise to a sort of implicit dissipation. Nevertheless, the model acts to bring the vertical temperature gradient in a more stable configuration and the Hadley circulation is in any case reproduced demonstrating the robustness of the model.

With n getting larger, the θ_E distribution becomes flatter in the tropical region and θ clamps to θ_E. In general, we expect that a vigorous circulation occurs in a fast rotating planet unless the thermal gradient becomes small in the tropics. In such a case the angular momentum homogenization is equivalent to a weakening of the rotation (Cessi, 1998). If the circulation is proportional to the cube of the meridional temperature gradient, it is quite evident that when such a gradient has high values the circulation is vigorously driven by this term, whereas when it approaches to zero it is the term $\theta_E - \theta$ dominates. ~~). The parameter *n* controls the Hadley cell and jet stream widths. The experiment with *n*=*k*=0.5 has Hadley cells and jet streams quite narrow. As far as the vertical position of the maximum value of the stream function is concerned, the experiments with *k*=0.5, 1 and 1.5 exhibit particular behavior with respect to the other experiments. The stream function has its maximum at upper levels. It is likely that such a combination of the parameters favors air to move to higher levels with respect to experiments with higher *k* values.~~

HH80 found that the edge of the Hadley cell was at the mid-latitudes when the planetary rotation was lower than that of the earth. Since this phenomenon is here observed for a wider ~~temperature~~forcing distribution, this common result may be attributed to a low efficiency in the process of homogenization of momentum and temperature.

In order to explain equable climates like those supposed to be occurred in Cretaceous and Eocene, Farrell (1990) formulated an axisymmetric model starting from the Held and Hou model and a forcing with *n*=2 and *k*=1 where the temperature gradients became flat because of a dissipation term. For high values of *n* the θ distributions are similar to those obtained by our forcing conditions. In some respects, flattening of forcing distributions is equivalent to have the same dissipation term in the Farrell (1990) model. The poleward shift of the subtropical jets was also observed by HH80 when increasing the vertical diffusion.

Figure 5 shows the stream function and the zonal wind speed for the experiments *n*=*k*=0.5 (Fig. 5a) and *n*=*k*=3 (Fig. 5b). The parameter *n* controls the Hadley cell and jet stream widths. The results show that such with *n*=*k*=0.5 the Hadley cell and jet streams are

Formattato: western, Giustificato, Rientro: Prima riga: 0,85 cm, SpazioPrima: 6 pt quite narrow. As far as the vertical position of the maximum value of the stream function is concerned, the experiments with k=0.5, 1 and 1.5 exhibit particular behavior with respect to the other experiments. The stream function has its maximum at upper levels. This is related to the different stratification imposed by the parameter k. Stratification with low values of k favor air to move to higher levels with respect to experiments with higher k values.

3.2 Time-dependent simulations

Formattato: Struttura + Livello:2 + Stile numerazione: 1, 2, 3, … + Comincia da:1 + Allineamento: A sinistra + Allinea a: 0 cm + Imposta un rientro di: 1,02 cm

Since heating depends on solar irradiation, it is of interest to analyze the solutions obtained by the annually periodic thermal forcing and to compare it with the steady solutions described previously in this paper. Starting from Eq. (7), we can formulate ~~a~~an equilibrium temperature distribution having the maximum heating off the equator at latitude ~~-~~y_0~~-:~~:

$$\theta_E = \frac{4}{3} - |y - y_0|^n + \frac{\Delta_V}{\Delta_H}\left(z^k - \frac{1}{2}\right).$$

(~~12~~10)

where y_0 in Eq. (~~9~~10) is dependent on time according to

$$y_0(t) = sin\left(\frac{\varphi_0 \pi}{180}\right) \cdot sin\left(\frac{2\pi t}{360 days}\right)$$

(~~13~~11)

where φ_0 is the maximum latitude off the equator where heating is maximum. Equations ~~12~~11 and ~~13~~12 are the same used by Fang and Tung (1999) with the choice of maximum extension of φ_0 consistent with the choice of Lindzen and Hou (1988), i.e. $\varphi_0 = 6$~~°.~~°. A prescribed equilibrium temperature varying seasonally makes the simulations more realistic. As described previously, here we will focus on the average and maximum values, in absolute terms, of the stream function and zonal speed obtained during 360 days of simulations. The averaged values are obtained in these cases by averaging the outputs obtained every 30 days, starting from the minimum corresponding to the summer Hadley cell in the boreal hemisphere.

The annual averages of the time-dependent and equinoctial circulations shows that maximum stream ~~function s~~functions and zonal wind speeds behave quite similarly ~~in the annual averages of the time-dependent and equinoctial circulations. Nevertheless the time-dependent solutions never attain the symmetric circulation obtained by averaging the single snapshots~~ (Fig. ~~7). Even the real earth circulation never reaches the mean~~6), nevertheless the instantaneous Hadley circulation~~, even because of eddies, but symmetric Hadley cells are visible in~~ almost never resembles the ~~average~~modeled circulation (Fang and Tung, 1999) as well as the real one (Dima and Wallace, 2003).

The maximum stream function is obtained here ~~by the~~when k=n=0.5 (Fig. ~~7a~~6a). In general, for ~~*k*~~*n*=0.5, we have stronger circulations and winds. ~~It has confirmed the tendency to a weaker~~ These simulations confirm the inverse relationship between stream function strength and ~~wind speed when *n* increases. However, the~~ *n*. The circulation strength expressed as annually averaged value is weaker when compared with that obtained in the ~~time-dependent solution~~equinoctial experiments, when n is low and k is high, otherwise it is only slightly stronger, but it is never twice as strong as that of the equinoctial solution as found by Fang and Tung (1999). When n=2 and k=1 ~~it appears more~~our results are consistent with ~~the results of~~those obtained by Walker and Schneider (2005) as discussed in the Subsect. ~~3.3. The maximum zonal wind speed shows a behavior slightly different from the stream function intensity; there is a clear dependence on *n* and *k*.~~3.3. For example, there is not an analog maximum when n=0.5 and k=3 found in the steady solution~~ and thus for other *k* values where~~

~~the stream function has a relative maximum. With high *k* value the static stability is high and the maximum of circulation confined to lower levels prevents air upwelling at the high levels. Thus, the transfer of momentum to high level is less effective with respect to the case *k*=0.5 where it is favored instead~~. The annually averaged maximum wind speed shows only a slight dependence on *k* when *k* is low.

Formattato: Inglese (Stati Uniti)

The meridional position and the height of the maximum stream function ~~maximum~~ ~~shows~~show that there is no clear dependency on *n* and *k* (Fig. ~~8~~7). The difference between the time-dependent simulations and the average of the ~~non time-dependent simulations~~ steady solutions is quite interesting. ~~-~~It is to be noticed that the latitude of the stream function maximum in the time-dependent solution is in the range of 12.5° and 16° (Fig. ~~8a~~7a), whereas in the equinoctial solutions the correspondent latitude is within a ~~-~~larger range. ~~It is probable that this narrow interval is due to the averaging operation.~~ The maximum stream function is located at higher levels, between 4500 and 6000 ~~for~~, when k is equal or less to one when and *n* is less than 2.5. Otherwise the maximum is positioned under ~~2500~~3000 m except ~~when *n*=3 and *k*=0.5~~ (Fig. ~~8b).~~7b). Although the averaged results seem interesting, they are impressively similar to those obtained by the steady experiments, they are obtained by averaging snapshots of the time-dependent simulations and thus a cautionary note should be made about these results.

More than the steady solution, it is evident that the height of the maximum stream function is lower when *k*=3. In the steady solution this phenomenon is not that evident. When *k*=3, the vertical gradient of ~~the potential temperature~~ θ_E is higher in upper levels making those levels more stable and it prevents, evidently more than the equinoctial solution, air from moving higher leaving circulation occurring at lower levels. The case *k*=3 is equivalent to imposing a “natural” sponge layer at the top of the model. Thus it does not come as a surprise that the maximum stream function is lower than those observed in simulations with other *k* values. This result is analogous to that of Walker and Schneider (2005) that removed the maximum stream function at higher levels found by Lindzen and Hou (1988) adopting a numerical sponge layer at the top of the model. A comparison with previous works of the simulations with *n*=2 and *k*=1 will be discussed in the Subsect. 3.3. On the contrary, with low *k* values, the presence of weaker θ_E gradient at upper levels favors air to move higher and the maximum stream function is observed at upper levels. There are more time-dependent simulations with respect to the steady solutions that exhibit this upper level maximum stream function.

The position of the jet stream is almost similar to the one observed in the steady solution. It is confined between 28° and 30°, with latitude of averaged jet remaining almost at the same place~~ or moving equatorward with *n*~~, except when *n*=3 the jets are located at about 44° confirming the abrupt transition of the jet stream position when *n*=3 already found for the equinoctial experiment. Fu and Lin (2011) suggest that the jets moved poleward of about 1° per decade in the last several years but Strong and Davis (2007) observed that Northern hemisphere subtropical jet shifted poleward over the east Pacific, while an equatorward shift of the subtropical jet was found over the Atlantic basin. Excluding the case *n*=3, all the other subtropical jets in the different experiments have the position of the maximum very close to one another and the shifting range is very limited. ~~However, when we use the jet latitude to define the edge of the Hadley cell, there is no significant shift but when *n*=3. This appears to be in contrast with the Held and Hou model.~~Thus, when a vigorous circulation occurs the jet location must be located at about 30°, whereas reducing too much the tropical gradient the process of homogenization becomes weaker like in a slow rotating planet and this is confirmed in the time-dependent solution. Both Tandon et al. (2013) and Kang and Polvani (2011) found a discrepancy in this area with the jets that do not follow the Hadley cell edge. In an axisymmetric model, defining the Hadley edge as a function of the stream function and connecting it to the jet location is problematic because of lacking of a zero value of the stream function.

Figure ~~9~~8 shows the annually averaged circulation for the same cases as shown in Fig. ~~6~~5, which is obtained by annually averaged heating. It is impressive how the steady and time-dependent solutions resemble each other. As in Fang and Tung (1999) the annual mean meridional circulation has the same extent, but differently from them the strength of the annual mean circulation of the time-dependent solution is almost the same of the steady solution.

When the heating center is off the equator the intensity of the winter cell is stronger, whereas the cell of the summer hemisphere is weak and sometimes almost absent. Figures ~~10 and 11 show~~9 shows the maxima of the stream function and zonal wind speed at the winter solstitial as a function of *n* and *k*. The maximum stream function as a function of *n* and *k* has the same configuration of the steady solution. Here, as expected the maximum intensity of the meridional circulation (Fig. ~~10a)~~9a) reached during the simulation is twice as strong as that of the steady solution~~.~~ or the annually averaged time dependent solution and it has about the same strength of the observed circulation. However the winds are much stronger too, in contrast with observations. The zonal wind has a different configuration instead, the maximum zonal wind speed is obtained when *n*=1 (Fig.~~11~~9b).

We can inspect a couple of simulations when the stream function reaches its maximum in the boreal hemisphere. Figure ~~12~~10 shows the stream function and the zonal wind speed when n=2 and k=0.5 (Fig. ~~12a~~10a, b) and n=2 and k=3 (Fig. ~~12 b~~10 c, d). When k=0.5 (upper panels) the boreal (winter) circulation is much stronger when k=0.5, with the austral (summer) circulation almost absent. The vertical extent is larger and the maximum is located at higher levels. The summer and winter jets are both more intense than their counterparts for k=3. The tropical easterly winds are in this case stronger than those for k=3 (13.8 ms^{-1} vs 11.4 ms^{-1}) and the easterly region is also wider. When k=3, it is noted that the ~~boreal~~winter cell is located closer to the equator than the ~~austral~~summer cell~~ (not easily visible in the figure when k=0.5).~~.

3.3 A discussion on the case *n*=2 *k*=1

Formattato: Struttura + Livello:2 + Stile numerazione: 1, 2, 3, … + Comincia da:1 + Allineamento: A sinistra + Allinea a: 0 cm + Imposta un rientro di: 1,02 cm

When n=2 and k=1, corresponding to the classic case discussed in many studies, we found that the time-dependent solution is only slightly stronger than the steady solution. Lindzen and Hou (1988) proposed a study of the Hadley circulation in which the maximum heating was 6° off the equator. In their non-time-dependent model, the solution showed an average circulation much stronger ~~by a factor 15 for $\phi_0 = 6°$~~with respect to the equinoctial solution.~~–~~ Lindzen and Hou (1988) suggested that this exceptional strength was due to a nonlinear amplification of the annually averaged response to seasonally varying heating, although Dima and Wallace (2003) in a study on the seasonality of the Hadley circulation did not observe any nonlinear amplification.

With the parameters used for equinoctial and time-dependent simulations we performed an experiment like that of Lindzen and Hou (1988), with $\phi_0 = 6°$ that will be referred to as solstitial experiment. We found that the winter circulation is stronger by a factor three with respect to the steady solution obtained with the equinoctial heating consistent with the result of the axisymmetric model in Walker and Schneider (2005). However, the average circulation~~,~~ obtained by averaging two solstitial experiments, with ~~-~~$\phi_0 = 6°$ and ~~-~~$\phi_0 = -6$~~°,~~°

respectively is only 1.5 times stronger than the steady solution with $\phi_0 = 0°$, and it has a maximum in the upper levels of the model domain as in Lindzen and Hou (1988). We suggest that this maximum is due to a numerical effect caused by averaging the single solstitial experiments rather than a spurious effect caused by the rigid lid as suggested in Walker and Schneider (2005), even though a sponge layer actually lowers ~~this~~the maximum stream function height and we can see the effects of a stronger vertical gradient in the upper levels especially in the time-dependent solution (cf Fig. 3 and Fig. ~~9).~~ 7). Single solstitial experiments did not show a maximum in upper levels and so the equinoctial and time-dependent experiments (~~Fig. 13~~Figs. 11a and 11b). Consequently the only operation performed to produce Fig. ~~13c~~11c, which exhibits the upper levels maxima, was to average the two solstitial experiments, which causes the maximum at upper levels.

Finally, we notice that comparing a time-dependent solution with $\varphi_0 = 6°$ with the equivalent steady solution having the heating off the equator is not properly correct, since for the time-dependent model φ_0 represents only the maximum extension of heating, hence a more correct comparison between time and no time-dependent solutions should be performed with the time-dependent solution having $\varphi_0 = 3°$. In such a case, the average solution is only slightly weaker than the Hadley circulation driven by annually averaged heating or by a time-dependent heating which does not show any maximum in the upper levels. Thus, the results of equinoctial, time-dependent and solstitial ($\varphi_0 = 3°$) experiments are mutually consistent.

4 Conclusions

Formattato: Struttura + Livello:1 + Stile numerazione: 1, 2, 3, … + Comincia da:1 + Allineamento: A sinistra + Allinea a: 0 cm + Imposta un rientro di: 0,76 cm

The ~~temperature distribution~~forcing of an Earth-like planet can change for several reasons. For instance, a change of ~~the temperature~~forcing distribution can be caused by different factors such as global warming or long-term variation of solar activity.

Under the assumption of an equal equator-pole difference at the surface we used an axisymmetric model to study the sensitivity of the tropical atmosphere to different ~~temperature~~θ_E distributions modulated by two parameters, n that controls the broadness of the distribution and k that modulates how the ~~temperature~~ θ_E is distributed vertically. Equinoctial and time-dependent solutions were simulated and compared. Moreover for the case n=2 and k=1, corresponding to the classical distribution used in literature, a few solstitial experiments were also run. When n=2 and k=1, the annually averaged circulation of equinoctial, time-dependent and solstitial experiments are quite close to one another, consistent with the results of Walker and Schneider (~~2006~~2005). However, the results differ from those of Lindzen and Hou (1988) and Fang and Tung (1999). As in all those works the maximum of the stream function of the solstitial experiment ~~appears to be~~is at upper levels, but it seems to be related to a spurious effect of the averaging operation rather than a spurious effect due to the rigid lid.

The results provide evidence that concentrated equilibrium temperature distributions enhance the meridional circulation and jet wind speed intensities, confirming findings of Lindzen and Hou (1988) even though these authors imposed the same energy input. However, in the present study the concentrated distribution at the equator has lower energy input.

The width of the Hadley cell is proportional to n, but when the cell width increases its intensity decreases. ~~The~~Poleward shift of the Hadley circulation with warming is very robust as it has been observed in many models and over large range of climates (Frierson et al., 2007). Since the equator-pole gradient is the same for all the experiments~~; hence~~ with the same k; it ~~is~~evident that the gradient ~~equator-subtropic that~~ in the tropical region controls the circulation strength. ~~Even k, hence the lapse rate,~~The term k controlling the imposed stratification has influence on the actual temperature distribution that can differ remarkably from θ_E distribution.

Vertical stratification is important in determining the position and intensity of the Hadley cell and jet when n is low, i.e. when for whereas k loses its importance when the ~~temperature~~θ_E distribution is wider. This latter result is consistent with results of Tandon et al. (2013) who found that the Hadley cell expansion and jet shift had relatively little sensitivity to the change ~~in~~of the lapse rate. Consequently, the subtropical jet stream intensities are controlled by the broadness of horizontal equilibrium temperature rather than the ~~vertical lapse rate~~stratification, with higher values of the jet when the thermal forcing is concentrated to the equator. ~~However, results show~~In the case of time dependent solution with n=0.5 (concentrated heating) and k takes the extreme values (0.5 and 3) the simulated maximum stream function has the same magnitude order of the observed stream function, ten times larger than that ~~the~~obtained in HH80 and with the reference simulation, even though with stronger winds too.

The jet stream position does not show any dependence with n and k, except when the ~~temperature~~ θ_E distribution is the widest (n=3); in such a case an abrupt change occurs and the maximum of the zonal wind jet is located at mid-latitudes~~.~~ (47° in steady solution and 44° in annually averaged time-dependent solution). This behavior can explained by using the analytic study of this model performed by Cessi (1998) claiming that when the meridional gradient becomes too small the process of homogenization of temperature and momentum occurs slowly and the circulation behaves as that of a slow rotating planet that exhibits poleward shift of the subtropical jets.

Formattato: Rientro: Prima riga: 0,85 cm

Acknowledgements

Helpful discussions with Antonio Speranza, Valerio Lucarini and Renato Vitolo are gratefully acknowledged. The author thanks two anonymous reviewers for their insightful comments on the paper, which helped to improve the manuscript.

References

Allen, R. J., Sherwood, S. C., Norris, J. R., and Zender, C. S.: Recent Northern Hemisphere tropical expansion primarily driven by black carbon and tropospheric ozone. Nature, 485, 350–354, 2012.

Caballero, R., Pierrehumbert, R. T., and Mitchell, J. L.: Axisymmetric, nearly inviscid circulations in non-condensing radiative-convective atmospheres. Q. J. Roy. Met. Soc., 134, 1269-1285, 2008.

Cessi, P.: angular momentum and temperature homogenization in the symmetric circulation of the atmosphere. J. Atmos. Sci., 55, 1997-2015, 1998.

Chen, G., Lu J., and Sun L.: Delineating the eddy–zonal flow interaction in the atmospheric circulation response to climate forcing: Uniform SST warming in an idealized aquaplanet Model. J. Atmos. Sci., 70, 2214–2233. doi:http://dx.doi.org/10.1175/JAS-D-12-0248.1, 2013.

Dima, I. M., and Wallace, J. M.: On the seasonality of the Hadley cell. J. Atmos. Sci., ~~60,~~ 60, 1522-1527, 2003.

Fang, M., and Tung, K. K.: Time-dependent nonlinear Hadley circulation. J. Atmos. Sci., 56, 1797-1807, 1999.

Formattato: Inglese (Stati Uniti)

Farrell, B. F.: 1990: Equable Climate Dynamics. J. Atmos. Sci., 47, 2986–2995. doi: http://dx.doi.org/10.1175/1520-0469(1990)047<2986:ECD>2.0.CO;2, 1990.

Frierson, D. M. W., Lu, J., Chen, G.: Width of the Hadley cell in simple and comprehensive general circulation models. Geophys. Res. Lett., L18804, 2007.

Fu, Q., Johanson, C. M., Wallace, J. M., and Reichler, T.: Enhanced mid-latitude tropospheric warming in satellite measurements. Science, 312, 1179, -2006.

Fu, Q., and Lin, P.: Poleward shift of subtropical jets inferred from satellite-observed lower stratospheric temperatures. J. Climate, 24, 5597-5603, doi:10.1175/JCLI-D-11-00027.1, 2011.

Gastineau, G., Le Treut, H. Li, L.: Hadley circulation changes under global warming conditions indicated by coupled climate models Tellus, 60, 863-884. doi:10.1111/j.1600-0870.2008.00344.x, 2008.

Gitelman, A. I., Risbey, J. S., Kass, R. E., and Rosen, R. D.: Trends in the surface meridional temperature gradient. Geophys. Res. Lett., 24, 1243–1246, 1997.

Greenwood, D. R. and Wing, S. L.: Eocene continental climates and latitudinal temperature gradients, Geology, 23, 1044–1048, 1995.

Held, I. M., and Hou, A. Y.: Nonlinear axially symmetric circulation in a nearly inviscid atmosphere. J. Atmos. Sci., 37, 515-533, 1980.

Hou, A.Y., and Lindzen, R. S.: The influence of concentrated heating on the Hadley circulation. *J. Atmos. Sci.*, **49**, 1233-1241, 1992.

Hu, Y., and Fu, Q.: Observed poleward expansion of the Hadley circulation since 1979. Atmos. Chem. Phys., 7, 5229–5236, 2007.

Johanson, C. M., and Fu, Q.: Hadley cell widening: Model simulations versus observations. J. Climate, 22, 2713– 2725, 2009.

Kang, S. M., and Polvani, L. M.: The interannual relationship between the latitude of the eddy-driven jet and the edge of the Hadley Cell. J. Climate 24 (2): 563–68.

doi:10.1175/2010JCLI4077.1, 2011.

Kim, H.-K., and Lee, S.: Hadley cell dynamics in a primitive equation model. Part II: Nonaxisymmetric flow. J. Atmos. Sci., 58, 2859–2871, 2001.

Lindzen, R. S., and Hou, A. Y.: Hadley circulations for zonally averaged heating centered off the Equator, J. Atmos. Sci., 2416-2427, 1988.

Liu, J., Song, M., Hu, Y., and Ren, X.: Changes in the strength and width of the Hadley Circulation since 1871. Clim. Past, 8, 1169–1175, doi:10.5194/cp-8-1169-2012, 2012.

Lu, J., Chen, G., and Frierson D. M. W.: Response of the zonal mean atmospheric circulation to El Niño versus global warming. J. Climate, 21, 5835–5851.doi: http://dx.doi.org/10.1175/2008JCLI2200.1, 2008.

Lu, J., Deser, C., and Reichler, T.: Cause of the widening of the tropical belt since 1958. Geophys. Res. Lett., 36, L03803, doi:10.1029/2008GL036076, 2009.

Lu, J., Vecchi, G. A., and Reichler T.: Expansion of the Hadley cell under global warming. Geophys. Res. Lett. 34, L06805, 2007.

Nguyen, H., Evans, A., Lucas, C., Smith, I., and Timbal, B.: The Hadley ~~Circulation~~circulation in ~~Reanalyses~~reanalyses: Climatology, ~~Variability~~variability, and ~~Change~~change. J. Climate, 26, 3357-3376, 2013.

Polvani, L. M., Waugh, D. W., Correa, G. J. P., and Son, S.-W.: Stratospheric ozone depletion: the main driver of 20th Century atmospheric circulation changes in the Southern Hemisphere. J. Climate, 24, 795-812, doi:10.1175/2010JCLI3772.1, 2011.

Santer, B. D., Thorne, P. W., Haimberger, L., Taylor, K. E., Wigley, T. M. L., Lanzante, J. R., Solomon, S., Free, M., Gleckler, P. J., Jones, P. D., Karl, T. R., Klein, S. A., Mears, C., Nychka, D., Schmidt, G. A., Sherwood, S. C., and Wentz, F. J.: Consistency of modelled and observed temperature trends in the tropical troposphere. Int. J. Climatol., 28 (13), 1703-1722, 2008.

Schaller, N., Cermak, J., Wild, M., and Knutti, R.: The sensitivity of the modeled energy budget and hydrological cycle to CO2 and solar forcing. Earth Syst. Dynam., 4, 253-266, doi:10.5194/esd-4-253-2013, 2013.

Schneider E. K.: Axially symmetric steady-state models of the basic state for instability and climate studies. Part II. Nonlinear calculations. J. Atmos. Sci., 34, 280-296, 1977.

Schneider, E. K., and Lindzen, R. S.: Axially symmetric steady state models of the basic state of instability and climate studies. Part I: Linearized calculations. J. Atmos. Sci., 34, 253-279, 1977.

Seidel, D. J., Fu, Q., Randel, W. J., and Reichler, T. J.: Widening of the tropical belt in a changing climate. Nat. Geosci., 1, 21–24, 2008.

Sherwood, S. C., Meyer, C. L., Allen, R. J., and Titchner, H. A.: Robust tropospheric warming revealed by iteratively homogenized radiosonde data. ~~Journal of~~J. Climate, 21 (20), 5336-5352, 2008.

Staten, P. W., Rutz, J., Reichler, T. and Lu, J.: Breaking down the tropospheric circulation response by forcing. Clim. Dynam., 39, 2361-2375, doi:10.1007/s00382-011-1267-y, 2011.

Strong, C., and Davis, R. E.: Winter jet stream trends over the Northern Hemisphere. Q. J. R. Meteorol. Soc. 133. 2109–2115, 2007.

Formattato: Inglese (Stati Uniti)

Formattato: Inglese (Stati Uniti)

Tandon, N. F., Gerber, E. P., Sobel, A. H. and Polvani, L. M.: Understanding Hadley Cell expansion versus contraction: Insights from simplified models and implications for recent observations. J. Climate 26 (12): 4304–21. doi:10.1175/JCLI-D-12-00598.1, 2013.

Titchner, H. A., Thorne, P.W., McCarthy, M.P., Tett, S. F. B., Haimberger L., and Parker, D. E.: Critically reassessing tropospheric temperature trends from radiosondes using realistic validation experiments. ~~Journal of~~J. Climate, 22 (3), 465-485, 2008.

Walker, C. C., and Schneider, T.: Response of idealized Hadley circulations to seasonally varying heating. Geophys. Res. Lett., 32, L06813, doi:10.1029/2004GL022304, 2005.

Walker, C. C., and Schneider, T.: Eddy influences on Hadley circulations: Simulations with an idealized GCM. J. Atmos. Sci., 63, 3333–3350, 2006.

~~Weliser~~Waliser, D. E., Shi, Z., Lanzante, J. R., and Oort, A. H.: The Hadley circulation: assessing NCEP/NCAR reanalysis ~~ans~~and sparse in situ estimates. Clim. Dyn., 15, 719-735, 1999.

Table 1. Latitudes (in degrees) of the maximum wind speed for the equinoctial and time-dependent solutions when k=1 as a function of the parameter *n*.

n	0.5	1	1.5	2	2.5	3
Equinoctial	27.4	28.7	27.4	26.1	28.7	47.7
Time dependent	28.7	28.7	28.7	27.4	27.4	44.4

Formattato: Tipo di carattere: Non Corsivo

Formattato: Tipo di carattere: Times New Roman, 12 pt, Colore carattere: Nero, Inglese (Stati Uniti)

Formattato: Normale

Figure Captions

Figure 1. Meridional (a) and vertical (b) ~~mean~~average of non-dimensional equilibrium temperature as a function of *n* ~~(panels~~ with k=1(a) and ~~b)~~k with n=0.5, 1 and ~~k (panel b)~~1.5 (b). Dimensional values are obtained multiplying by θ_0=300 K.

Figure 2. Maximum non-dimensional stream function (a) and zonal wind speed [ms^{-1}] (b) as function of parameters n and k for the steady solution. Dimensional values of the stream function are obtained multiplying by $\nu_V R\varepsilon^{-1} = 484$ m^{2}s^{-1}.

Formattato: Tipo di carattere: Corsivo

Formattato: Tipo di carattere: Corsivo

Figure 3. Latitude [degree] (a) and Height [m] (b) of maximum non-dimensional stream function.

Figure 4. ~~Relationship between Rossby number and poleward boundary of the Hadley cell as given by Eq. 10,~~ ~~$y_H = \sin\varphi_H$.~~

~~Figure 5.~~ Vertically averaged ~~potential temperature~~the θ (blue line) and θ_E (red line) for the ~~simulation~~simulations with n=~~k=~~3 and k=0.5 (a), k=1 (b) and k=3 (c). Dimensional values are obtained multiplying by θ_0=300 K.

~~Figure 6.~~Figure 5. Non-dimensional stream function (~~a and c~~contours) and zonal wind speed ~~(b and d~~[ms^{-1}] (colors) for the steady cases n=0.5, k=0.5 (~~upper panels~~a) and n=3, k=3 (~~lower panels).~~b). Dimensional values of the stream function are obtained multiplying by $\nu_V R\varepsilon^{-1} = 484$ m^{2}s^{-1}.

~~Figure 7.~~Figure 6. Maximum of annually averaged non dimensional stream function (a) and zonal wind speed [ms^{-1}] (b) as function of parameters n and k for the time-dependent simulations. Dimensional values of the stream function are obtained multiplying by $\nu_V R\varepsilon^{-1} = 484$ m^{2}s^{-1}.

Formattato: Tipo di carattere: Corsivo

Formattato: Tipo di carattere: Corsivo

Figure ~~8~~7. Latitude [degree] (a) and Height [m] (b) of maximum annually averaged non-dimensional stream function for the time-dependent solution.

Figure ~~9~~8. Annually averaged non-dimensional stream function (~~a and c~~contours) and zonal wind speed ~~(b and d~~[ms^{-1}] (colors) for the steady cases n=0.5, k =0.5 (~~upper panels~~a) and n=3, k=3 (~~lower panels).~~b). Dimensional values of the stream function are obtained multiplying by $\nu_V R\varepsilon^{-1} = 484$ m^{2}s^{-1}.

Figure 9. ~~Figure 10.~~ Maximum of non-dimensional stream function (a) and zonal wind speed [ms^{-1}] (b) ~~-~~as function of parameters n and k for the time-dependent simulations.

~~Figure 11. Latitude [degree] (a) and Height [m] (b)~~ Dimensional values of ~~maximum non-dimensional~~ the stream function ~~for the time dependent solution~~are obtained multiplying by $\nu_V R\varepsilon^{-1} = 484$ m^{2}s^{-1}.

~~Figure 12. Winter~~Figure 10. Boreal winter circulation, non-dimensional stream function (a and c) and zonal wind speed [ms^{-1}] (b and d) ~~when~~ for the time-dependent simulation with *n*=2, *k*=0.5 (upper panels) and *n*=2, *k*=3 (lower panels~~) for the time-dependent simulation~~). Dashed lines indicate negative values. Dimensional values of the stream function are obtained multiplying by $\nu_V R\varepsilon^{-1} = 484$ m^{2}s^{-1}.

Figure ~~13~~11. Non-dimensional ~~annually averaged~~ stream function (~~a,c,e~~contours) and zonal wind speed ~~(b,d,f~~ms^{-1}] (colors) when *n*=2 and *k*=1 for the steady solution (a), annually averaged for the time-dependent solution (b) and ~~with the~~averaged for maximum heating 6° off the equator (c). Dimensional values of the stream function are obtained multiplying by $\nu_V R\varepsilon^{-1} = 484$ m^{2}s^{-1}.

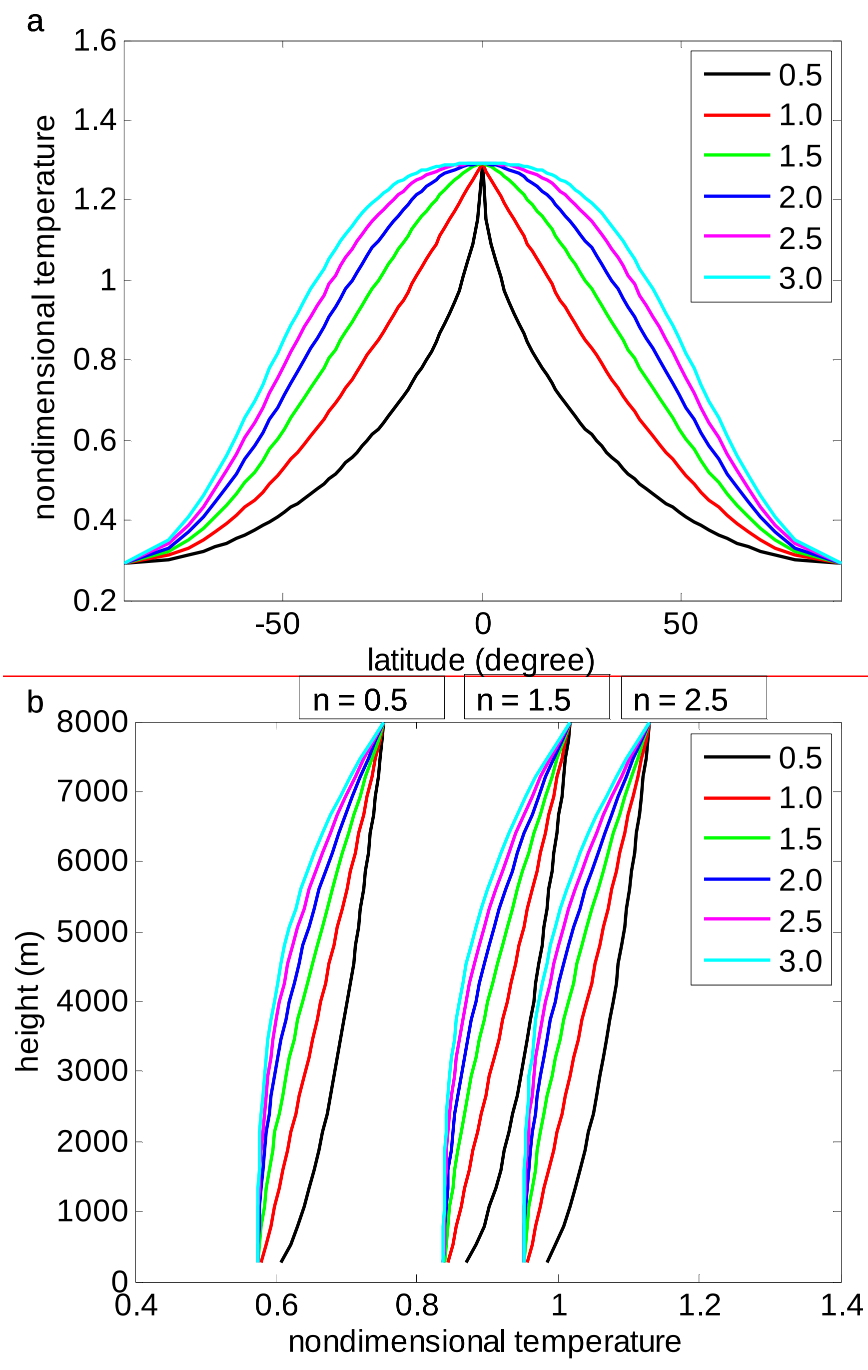
a
nondimensional temperature
latitude (degree)
0.5
1.0
1.5
2.0
2.5
3.0
b
n = 0.5
n = 1.5
n = 2.5
height (m)
nondimensional temperature

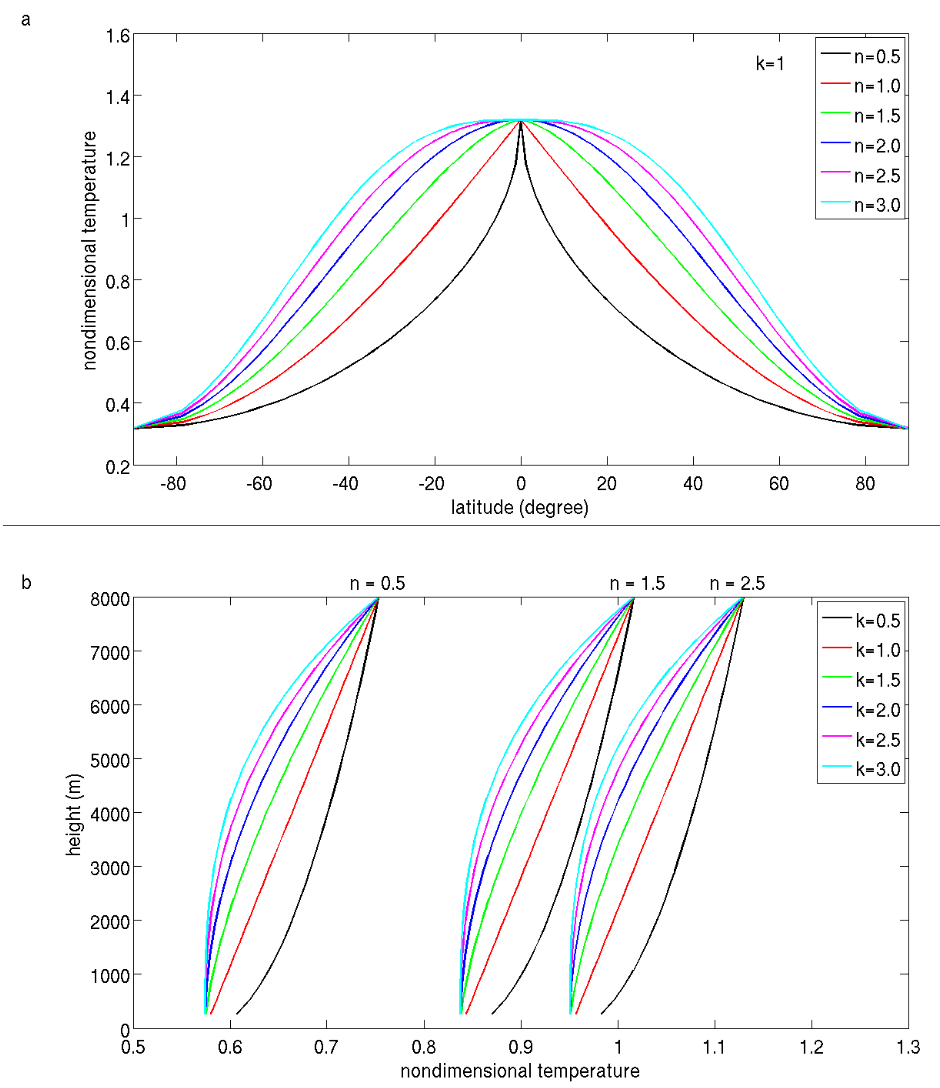
a
k=1
n=0.5
n=1.0
n=1.5
n=2.0
n=2.5
n=3.0
nondimensional temperature
latitude (degree)
b
n = 0.5
n = 1.5
n = 2.5
k=0.5
k=1.0
k=1.5
k=2.0
k=2.5
k=3.0
height (m)
nondimensional temperature

Figure 1.

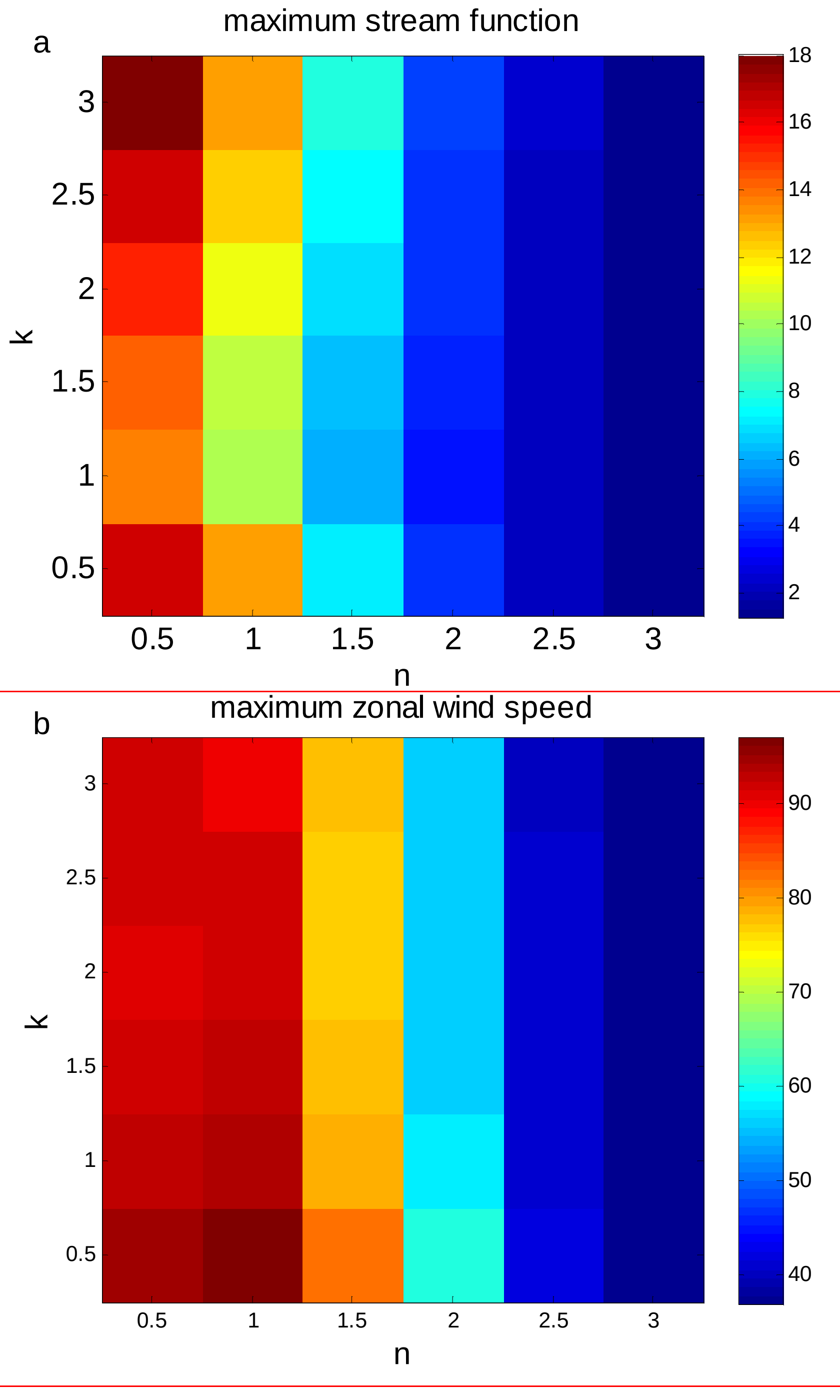
a
maximum stream function
k
n
0.5
1
1.5
2
2.5
3
18
16
14
12
10
8
6
4
2
b
maximum zonal wind speed
k
n
0.5
1
1.5
2
2.5
3
90
80
70
60
50
40

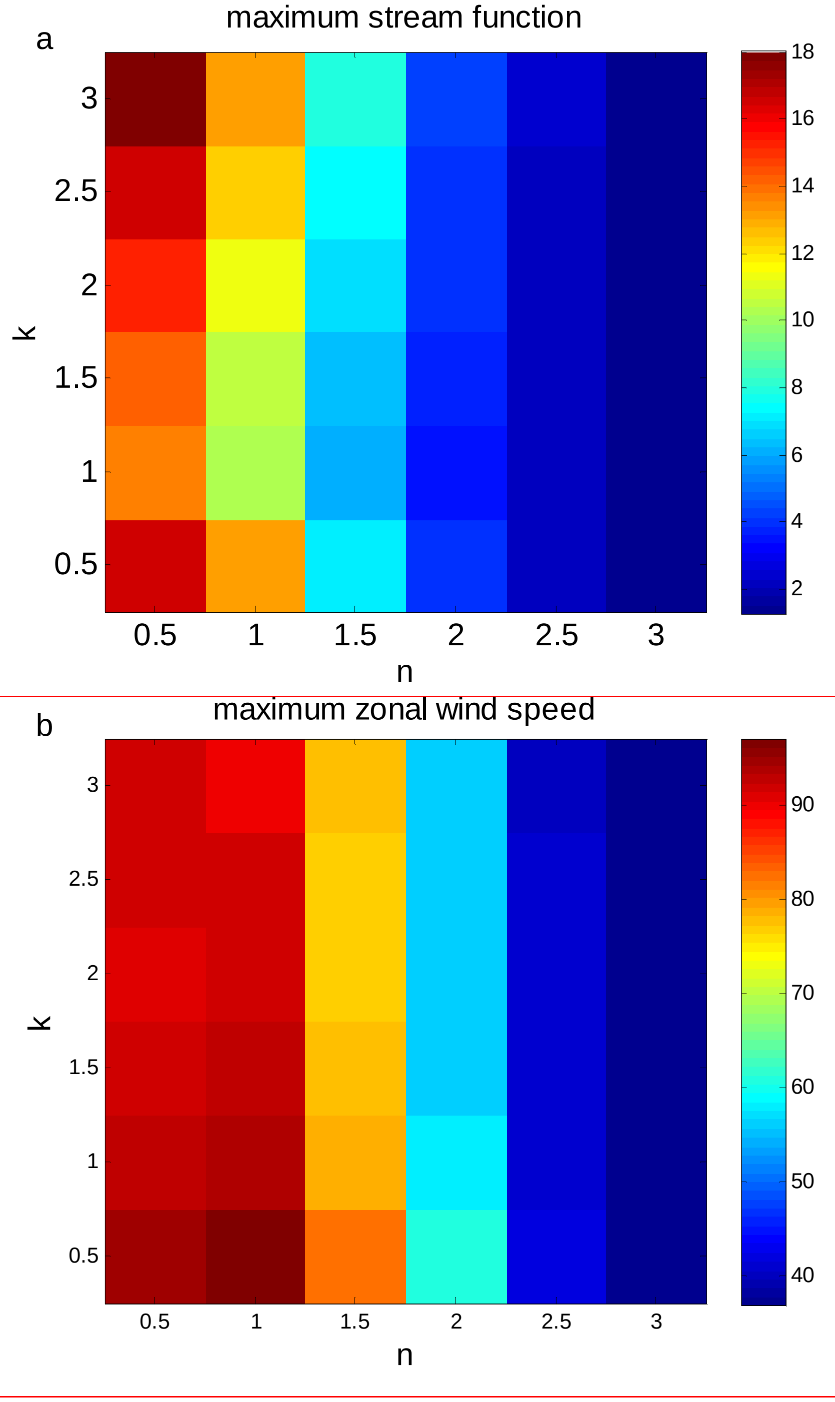
a
maximum stream function
k
n
3
2.5
2
1.5
1
0.5
0.5
1
1.5
2
2.5
3
18
16
14
12
10
8
6
4
2
b
maximum zonal wind speed
k
n
3
2.5
2
1.5
1
0.5
0.5
1
1.5
2
2.5
3
90
80
70
60
50
40

Figure 2.

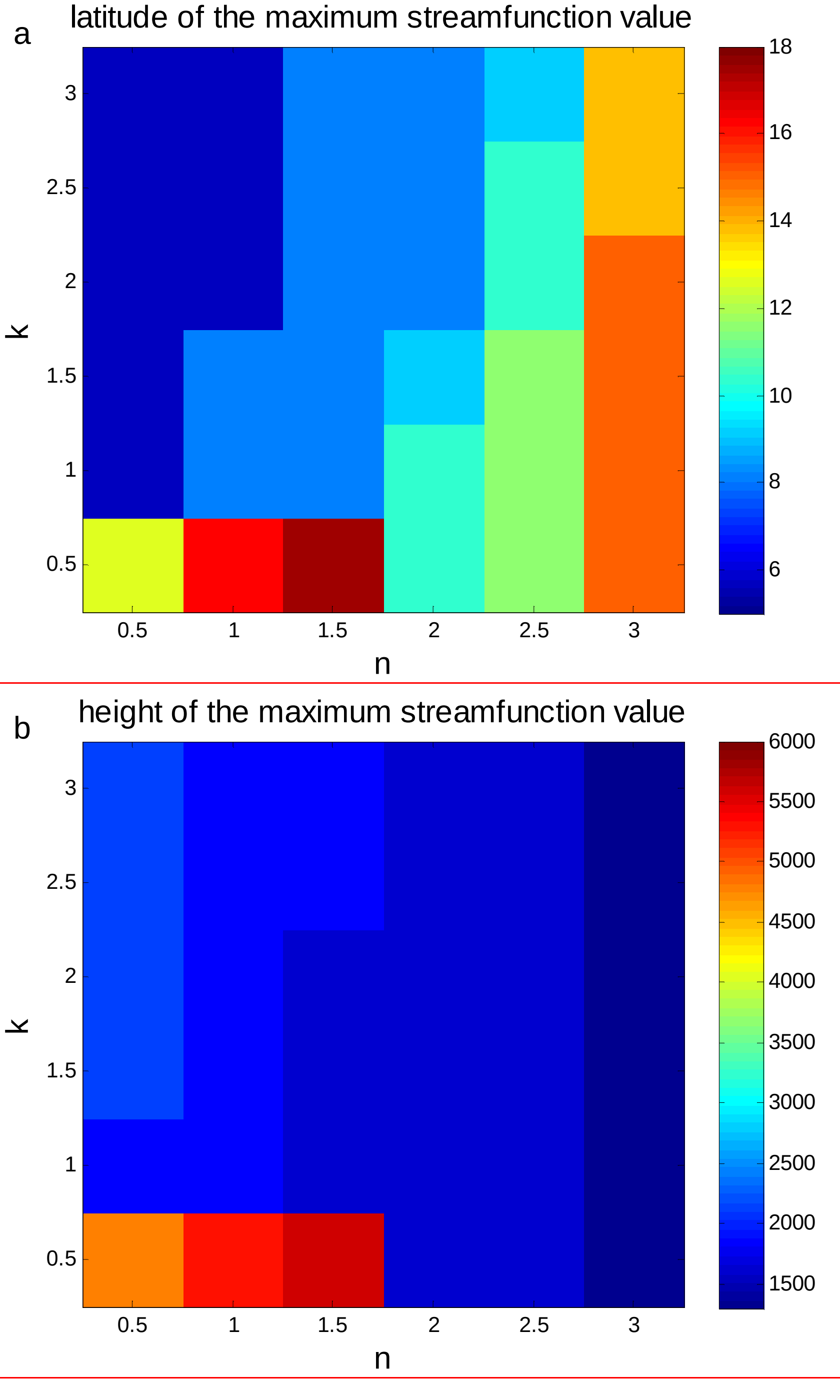
a
latitude of the maximum streamfunction value
k
n
0.5
1
1.5
2
2.5
3
6
8
10
12
14
16
18
b
height of the maximum streamfunction value
1500
2000
2500
3000
3500
4000
4500
5000
5500
6000

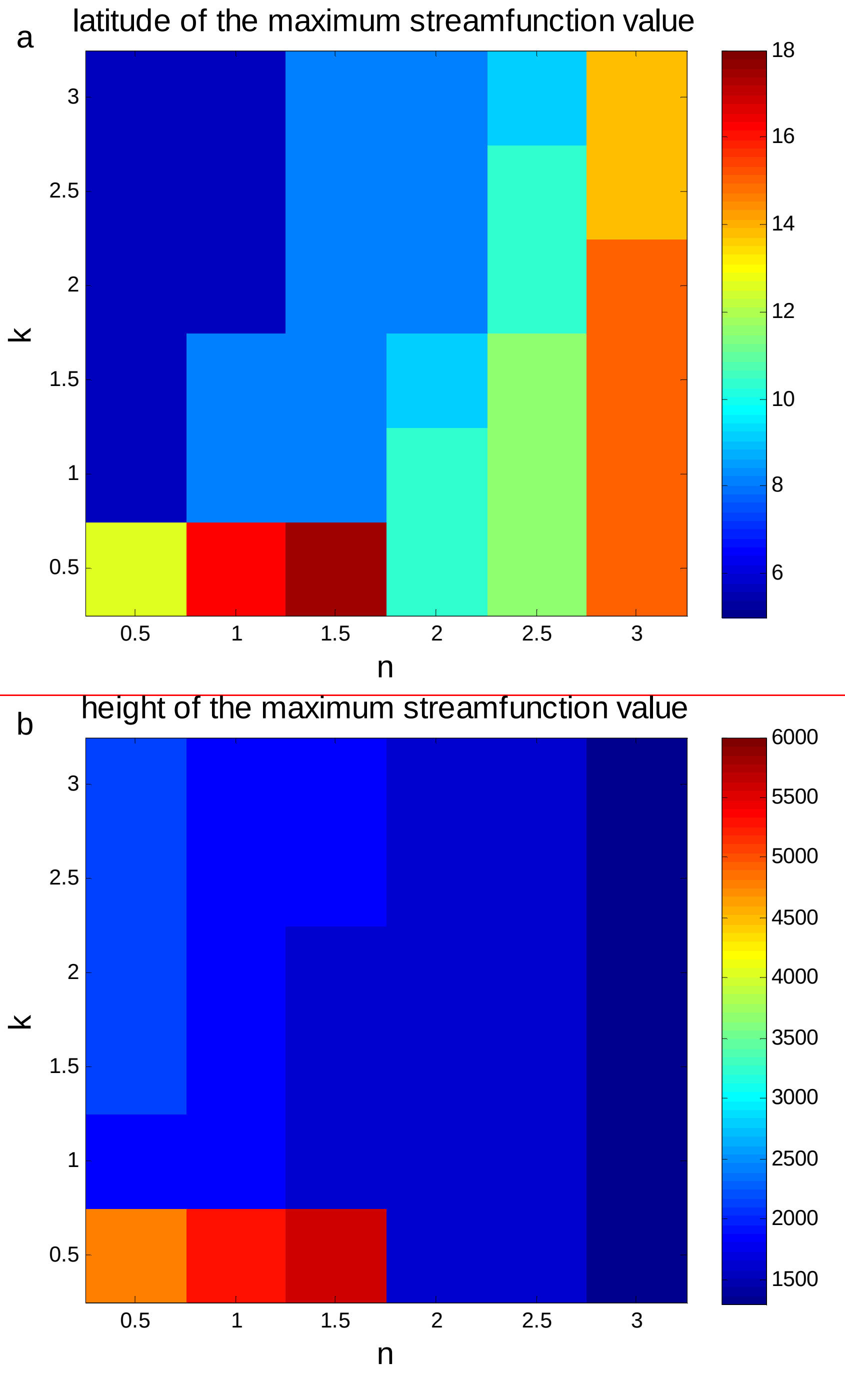
a
latitude of the maximum streamfunction value
k
3
2.5
2
1.5
1
0.5
n
0.5
1
1.5
2
2.5
3
18
16
14
12
10
8
6
b
height of the maximum streamfunction value
k
3
2.5
2
1.5
1
0.5
n
0.5
1
1.5
2
2.5
3
6000
5500
5000
4500
4000
3500
3000
2500
2000
1500

Figure 3.

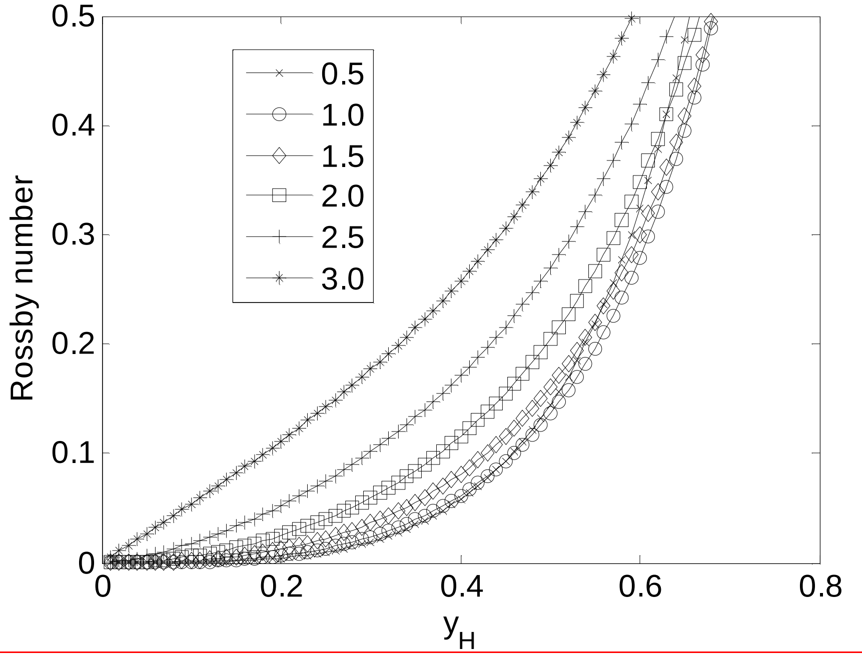

0.5
0.4
0.3
0.2
0.1
0
Rossby number
0.5
1.0
1.5
2.0
2.5
3.0
0
0.2
0.4
0.6
0.8
y_H

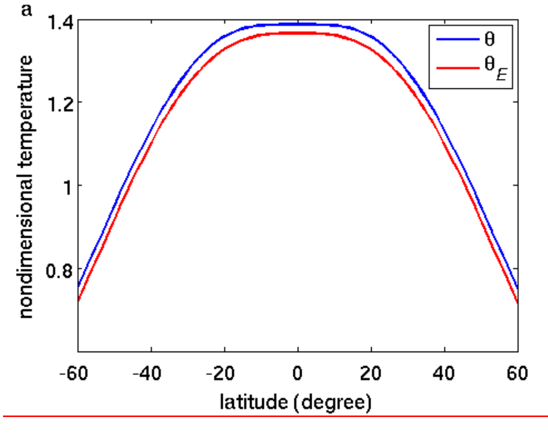

a
1.4
1.2
1
0.8
nondimensional temperature
θ
θ_E
-60
-40
-20
0
20
40
60
latitude (degree)

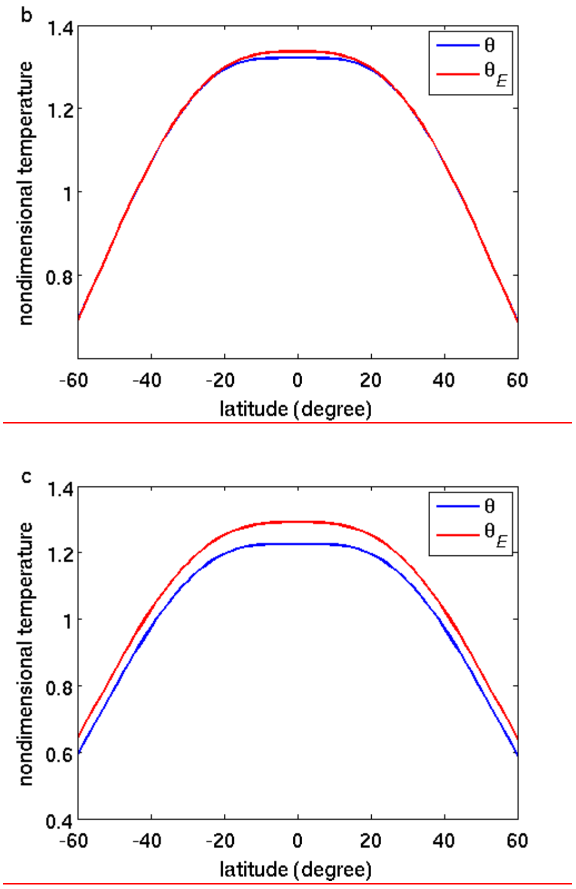
b
nondimensional temperature
latitude (degree)
θ
θ_E
c
nondimensional temperature
latitude (degree)
θ
θ_E

Figure 4.

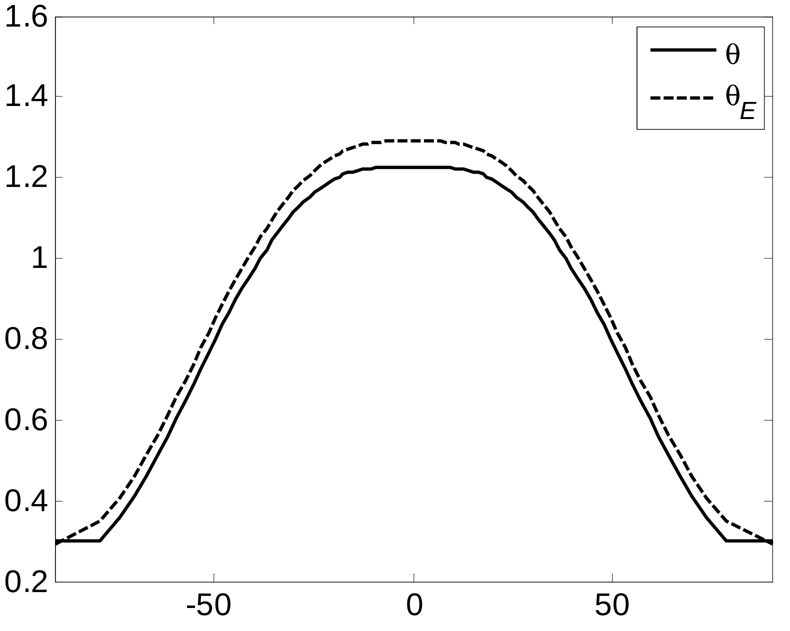
1.6
1.4
1.2
1
0.8
0.6
0.4
0.2
-50
0
50
θ
θ_E

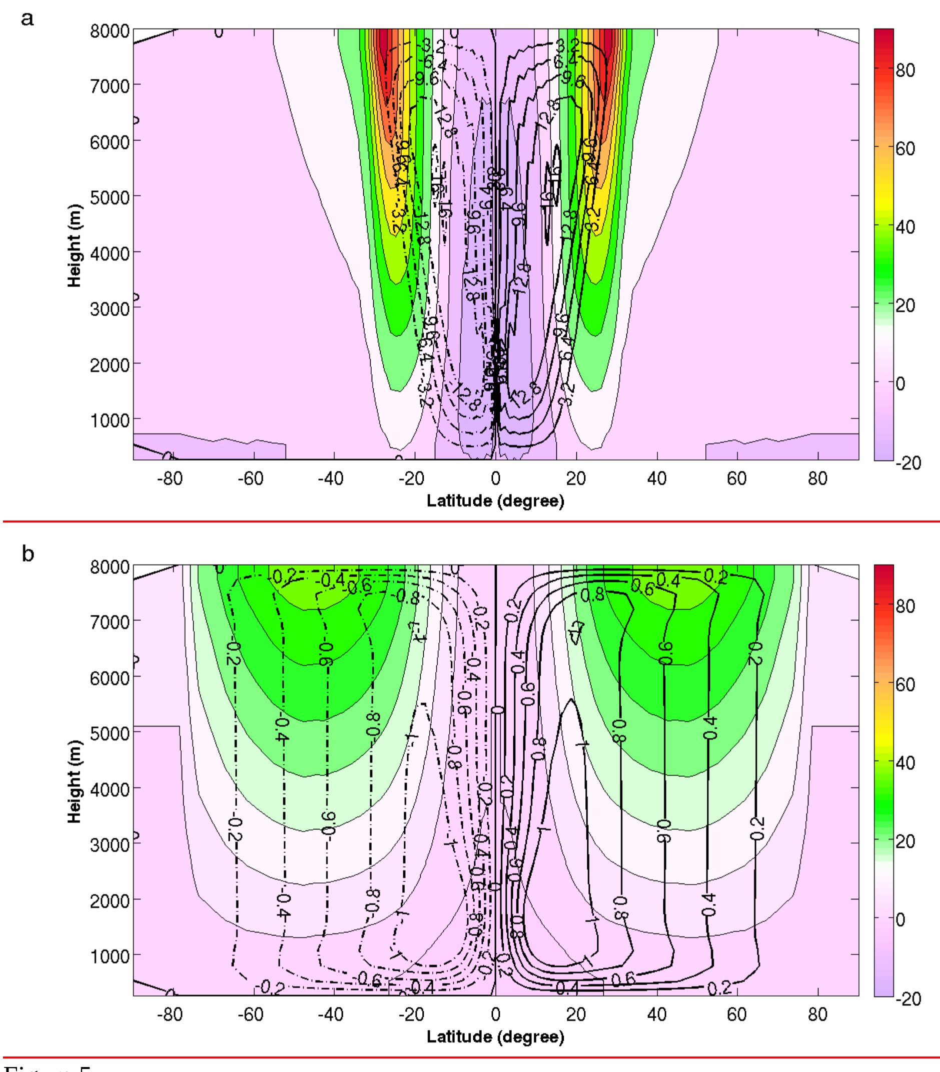

Figure 5.

Formattato: Normale

Formattato: Tipo di carattere: Times New Roman, 12 pt, Inglese (Stati Uniti)

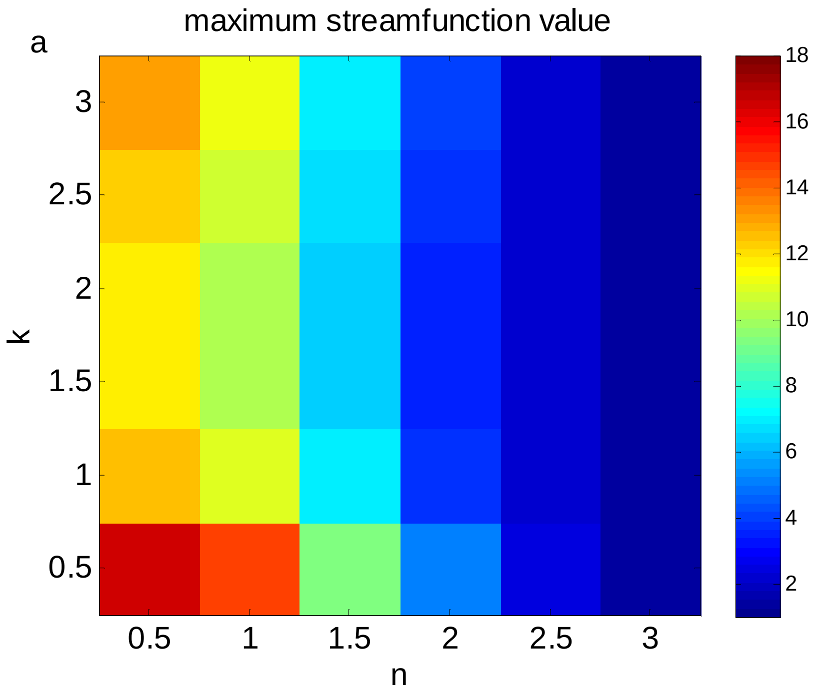

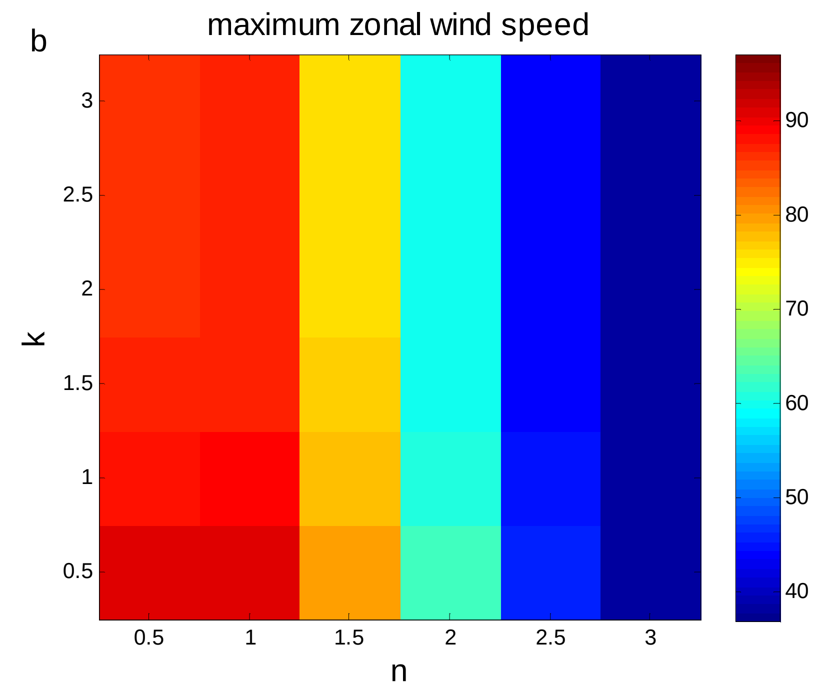

Formattato: Inglese (Stati Uniti)

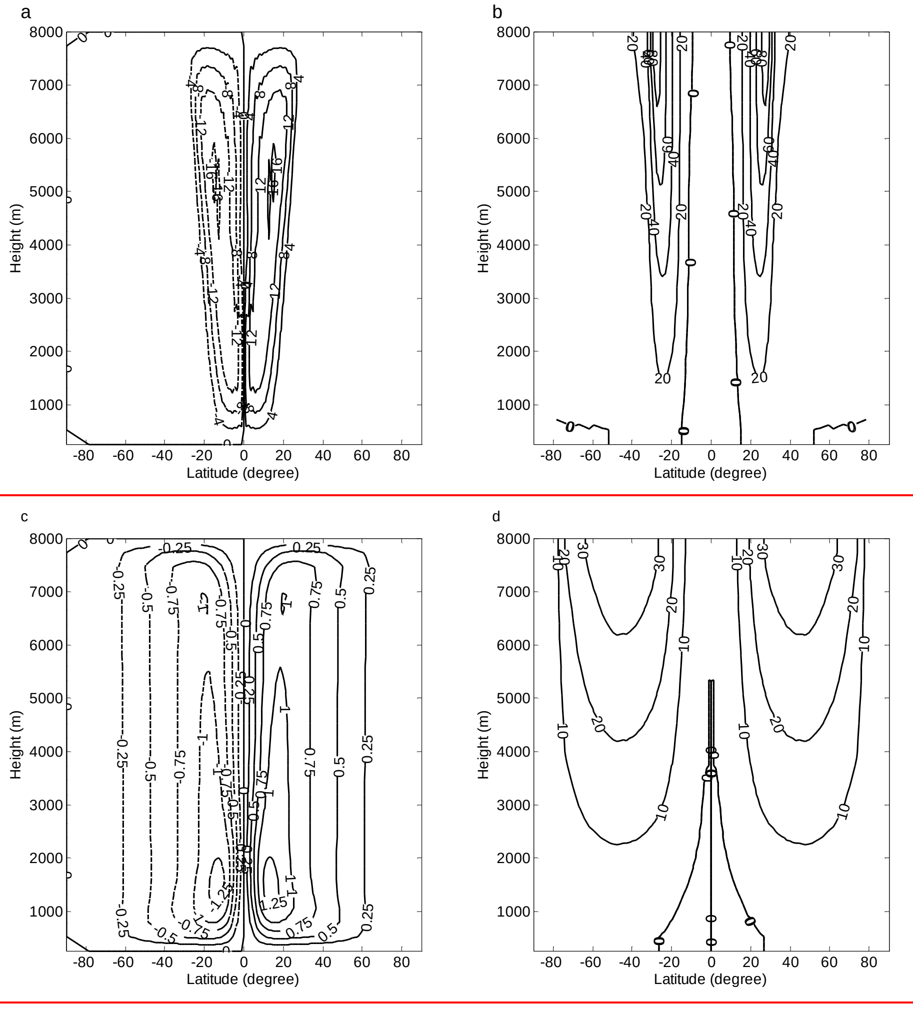

Figure 6.

Formattato: Tipo di carattere: Times New Roman

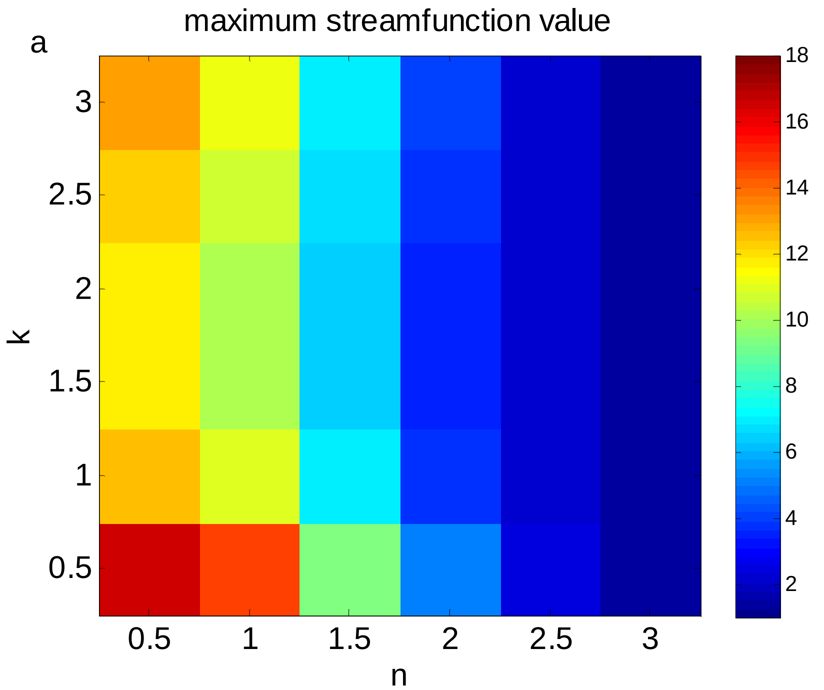

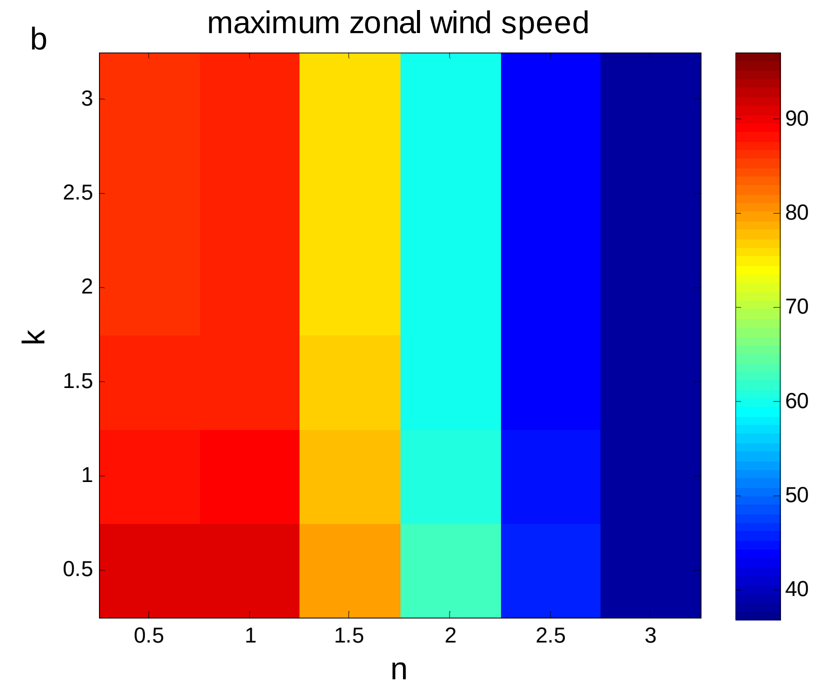

Formattato: Tipo di carattere: Times New Roman

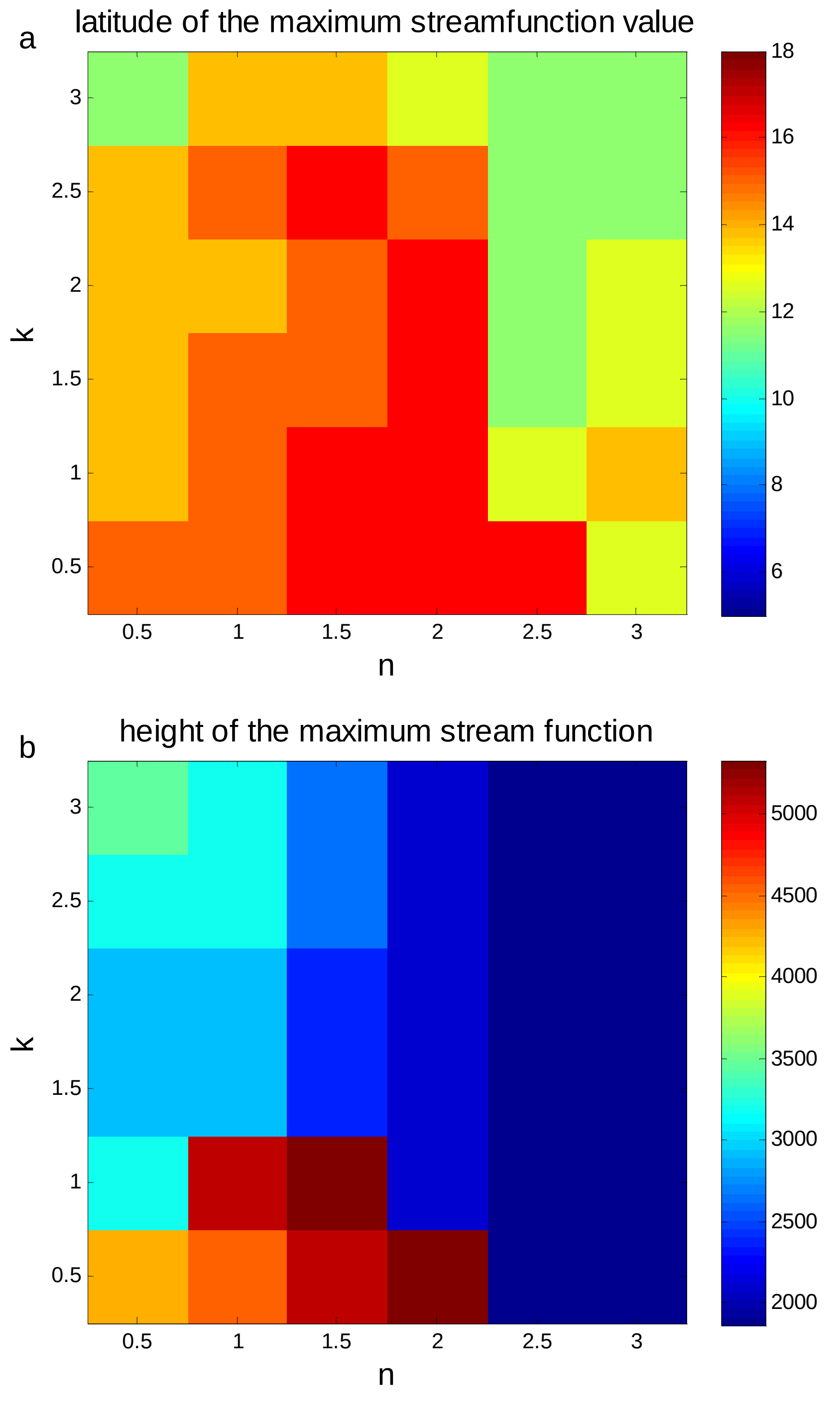
a
latitude of the maximum streamfunction value
k
n
b
height of the maximum stream function
k
n

1

2 Figure 7.

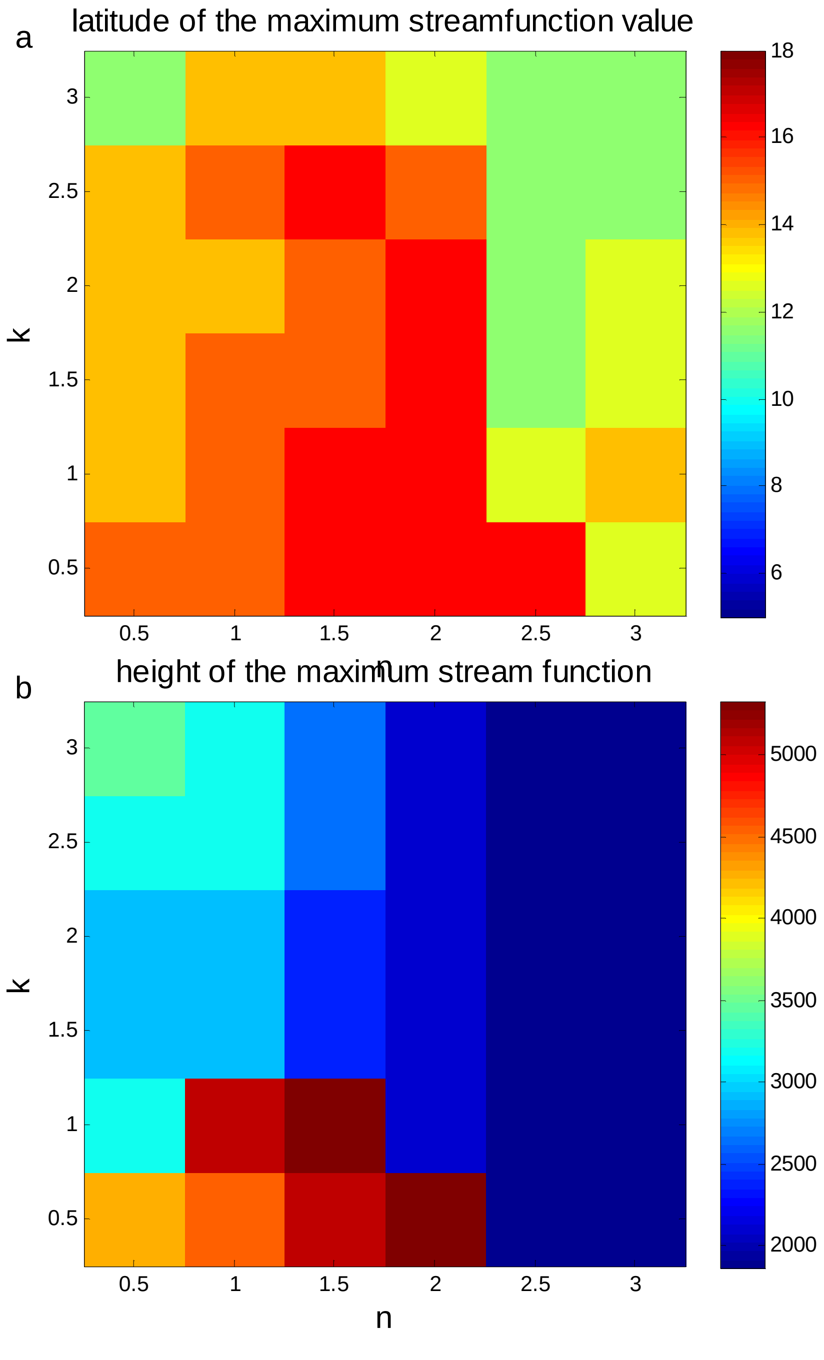
a
latitude of the maximum streamfunction value
k
n
0.5
1
1.5
2
2.5
3
18
16
14
12
10
8
6
b
height of the maximum stream function
k
n
5000
4500
4000
3500
3000
2500
2000

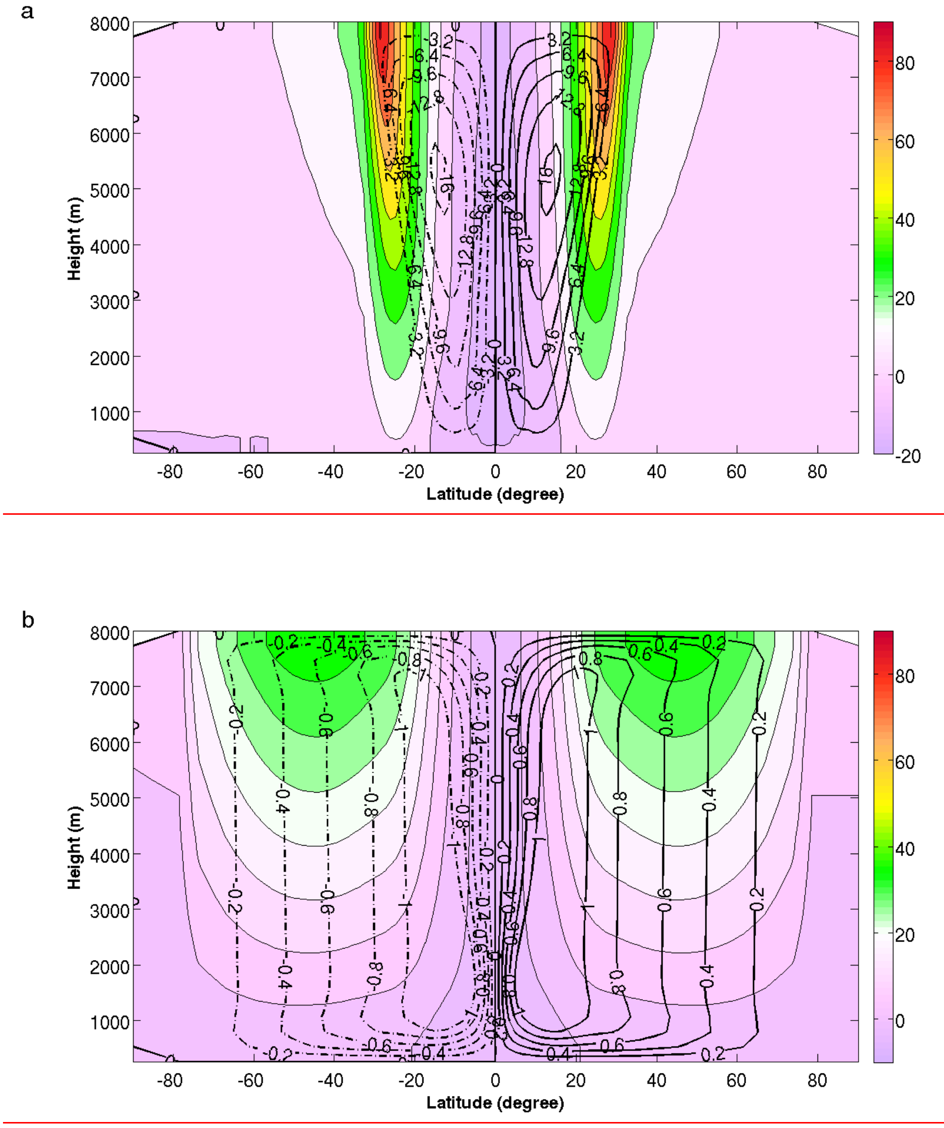

Figure 8.

Formattato: Tedesco (Germania)

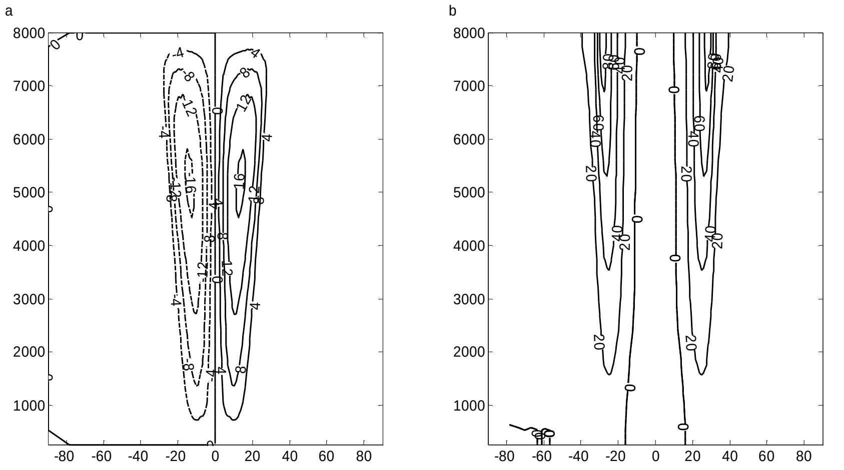
a
b
8000
7000
6000
5000
4000
3000
2000
1000
-80 -60 -40 -20 0 20 40 60 80

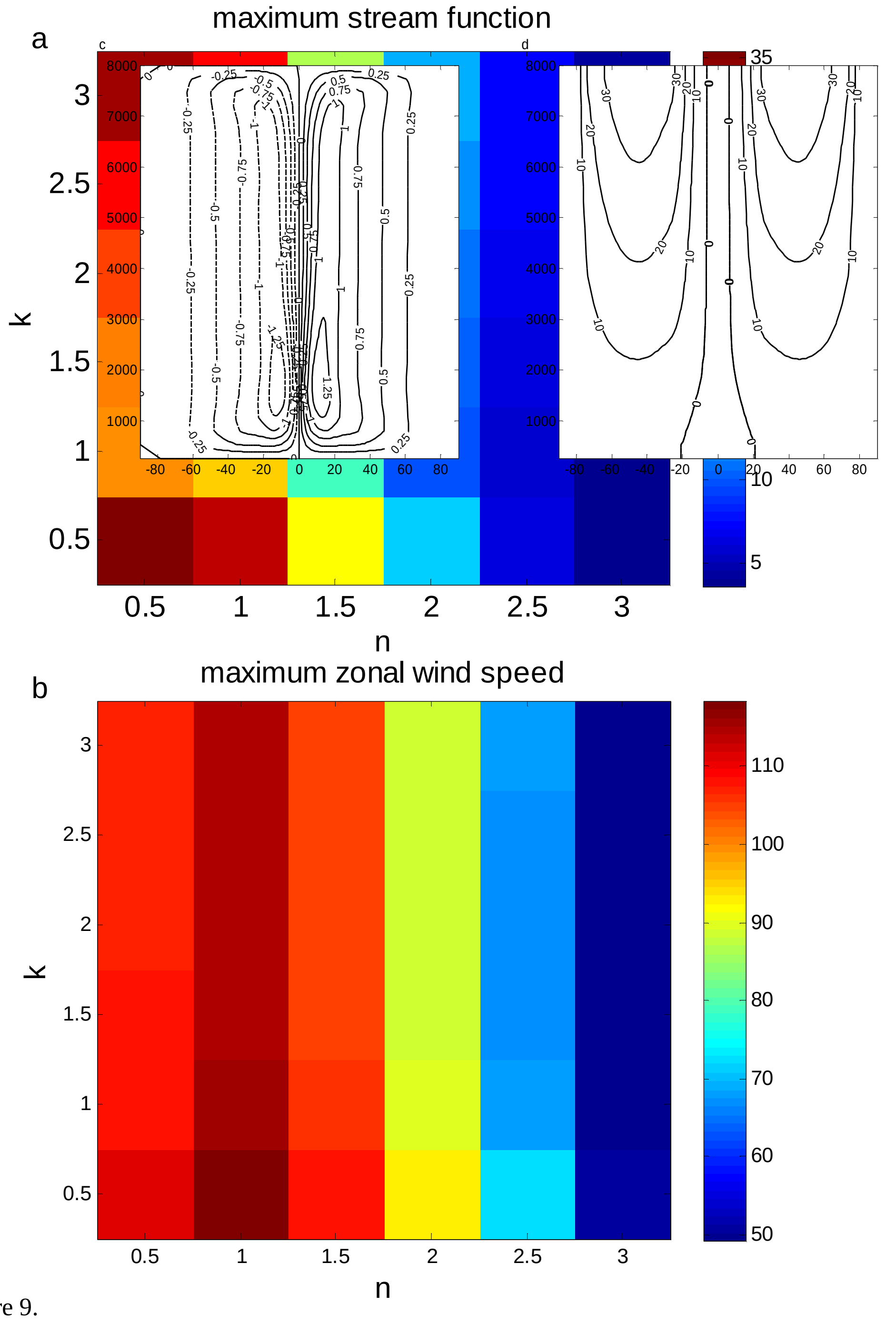
a
maximum stream function
k
n
c
d
b
maximum zonal wind speed
k
n

Figure 9.

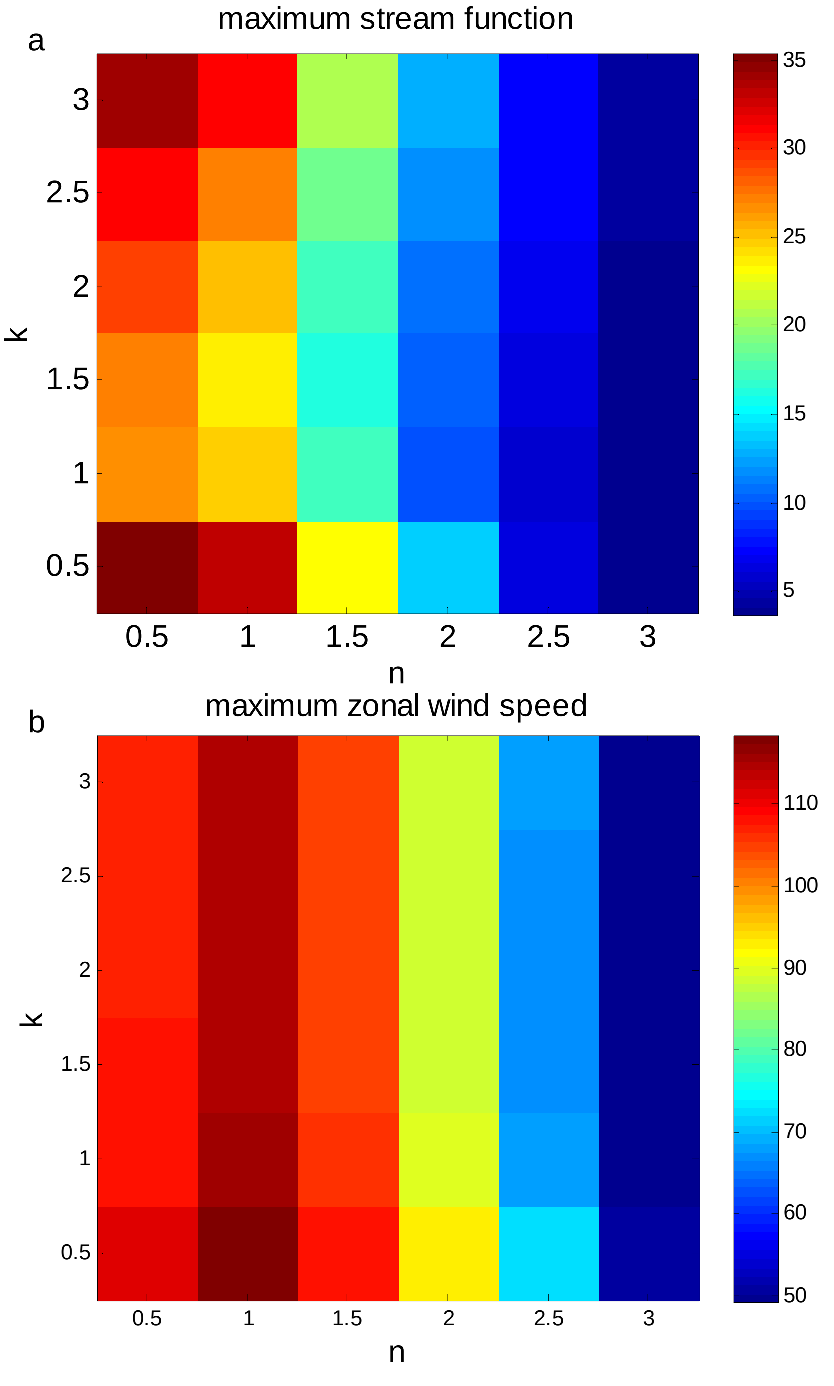
a
maximum stream function
k
3
2.5
2
1.5
1
0.5
0.5
1
1.5
2
2.5
3
n
35
30
25
20
15
10
5
b
maximum zonal wind speed
k
3
2.5
2
1.5
1
0.5
0.5
1
1.5
2
2.5
3
n
110
100
90
80
70
60
50

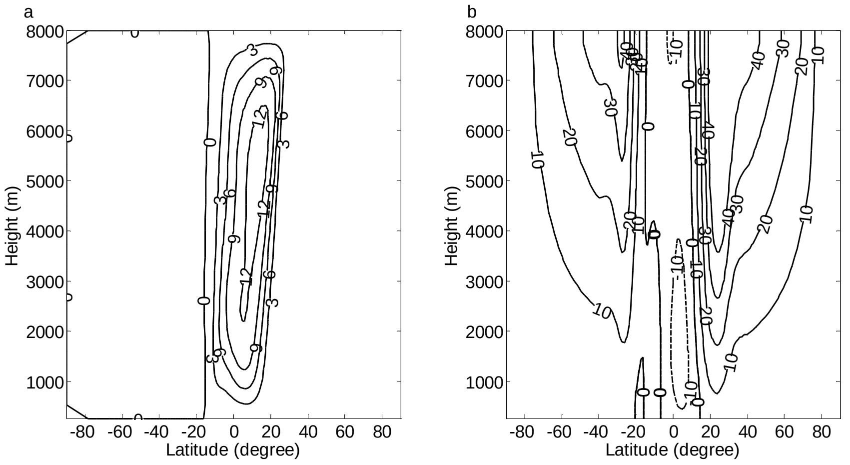
a
b
Height (m)
Latitude (degree)

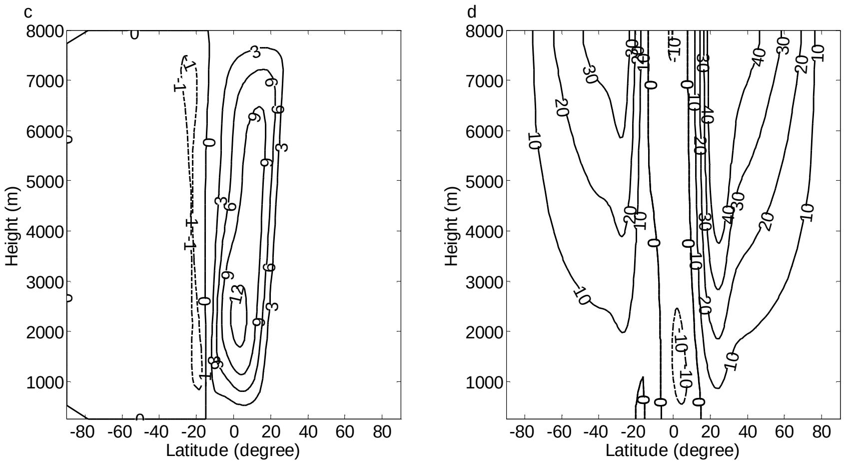
c
d
Height (m)
Latitude (degree)

Figure 10.

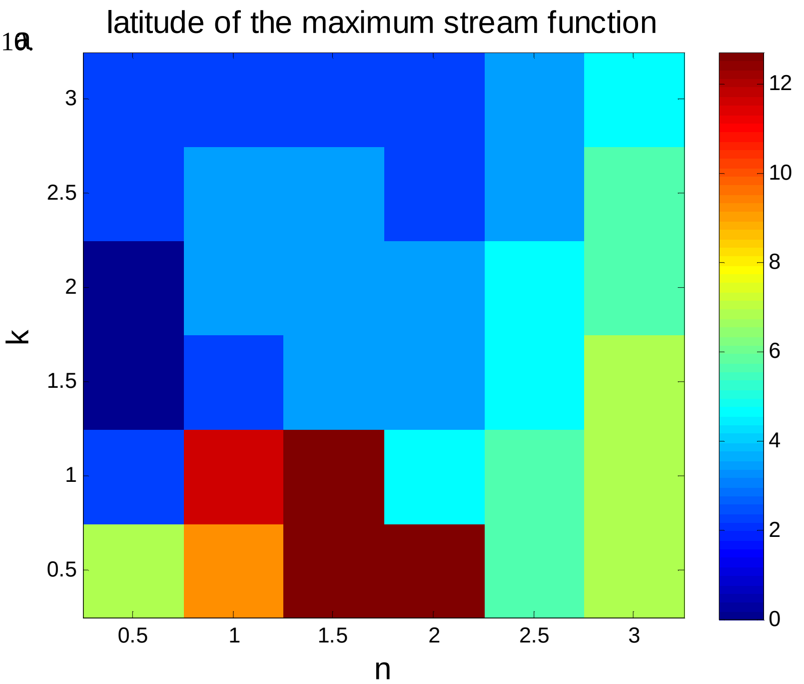
latitude of the maximum stream function
k
n

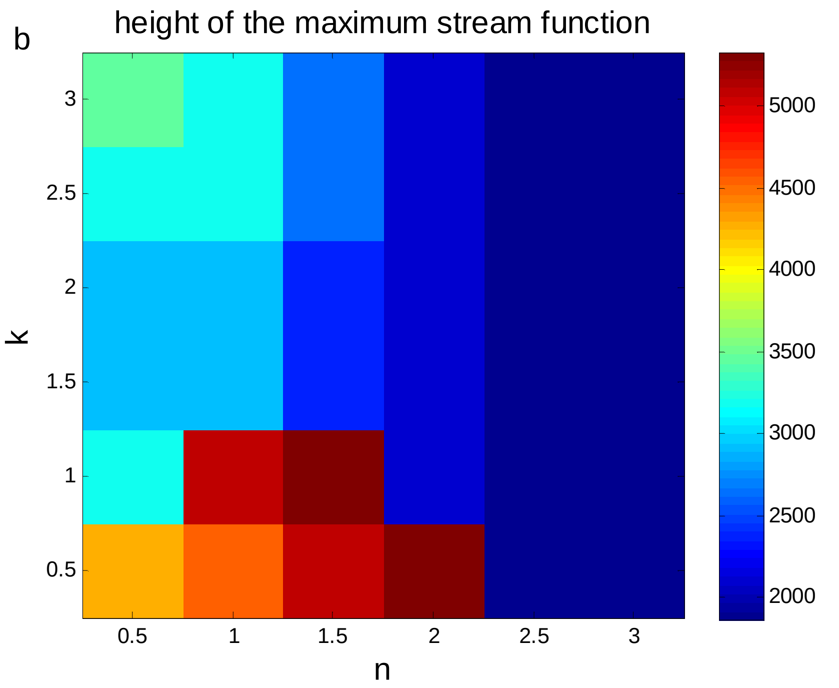
b
height of the maximum stream function
k
n
0.5
1
1.5
2
2.5
3
5000
4500
4000
3500
3000
2500
2000

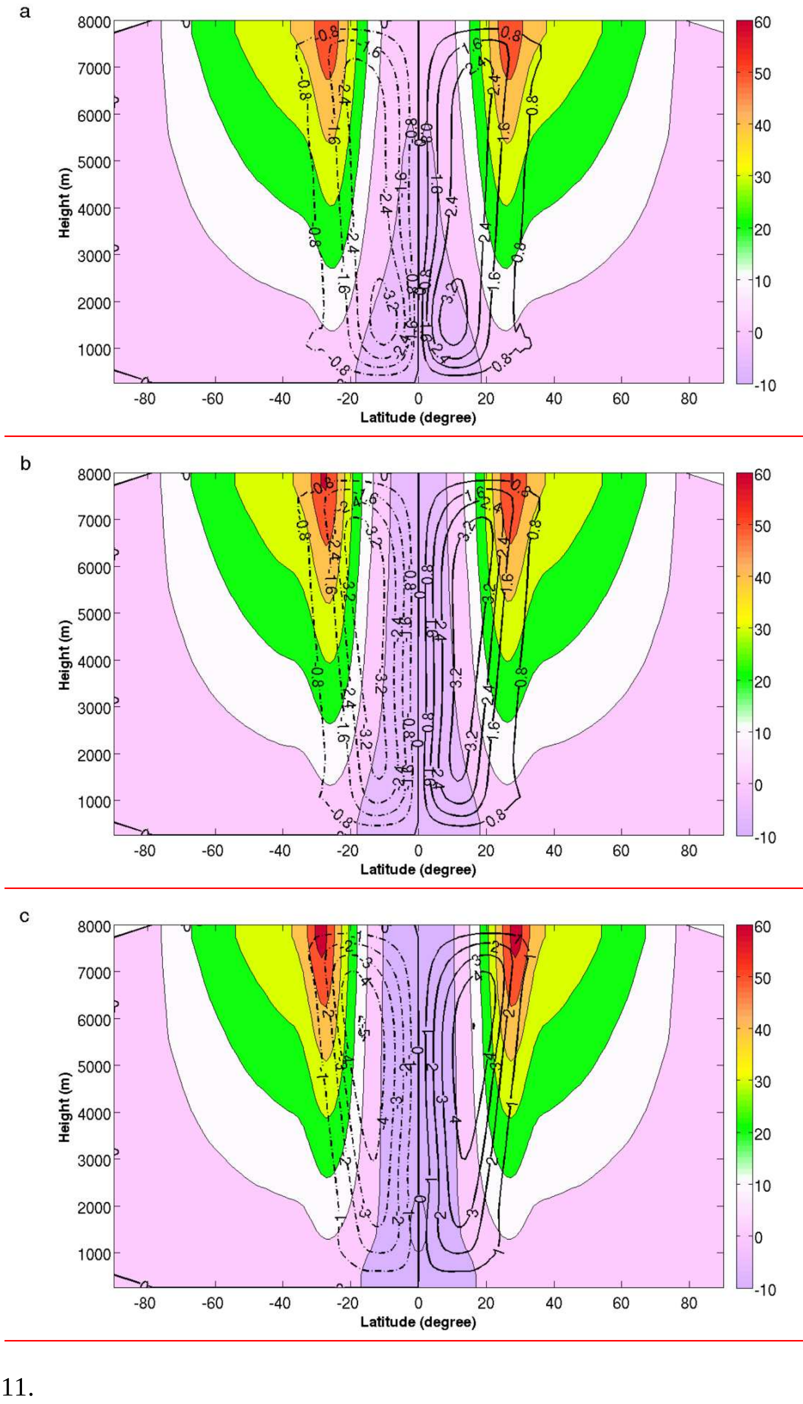
a
b
c
Height (m)
Latitude (degree)
8000
7000
6000
5000
4000
3000
2000
1000
-80
-60
-40
-20
0
20
40
60
80
60
50
40
30
20
10
0
-10

Figure 11.

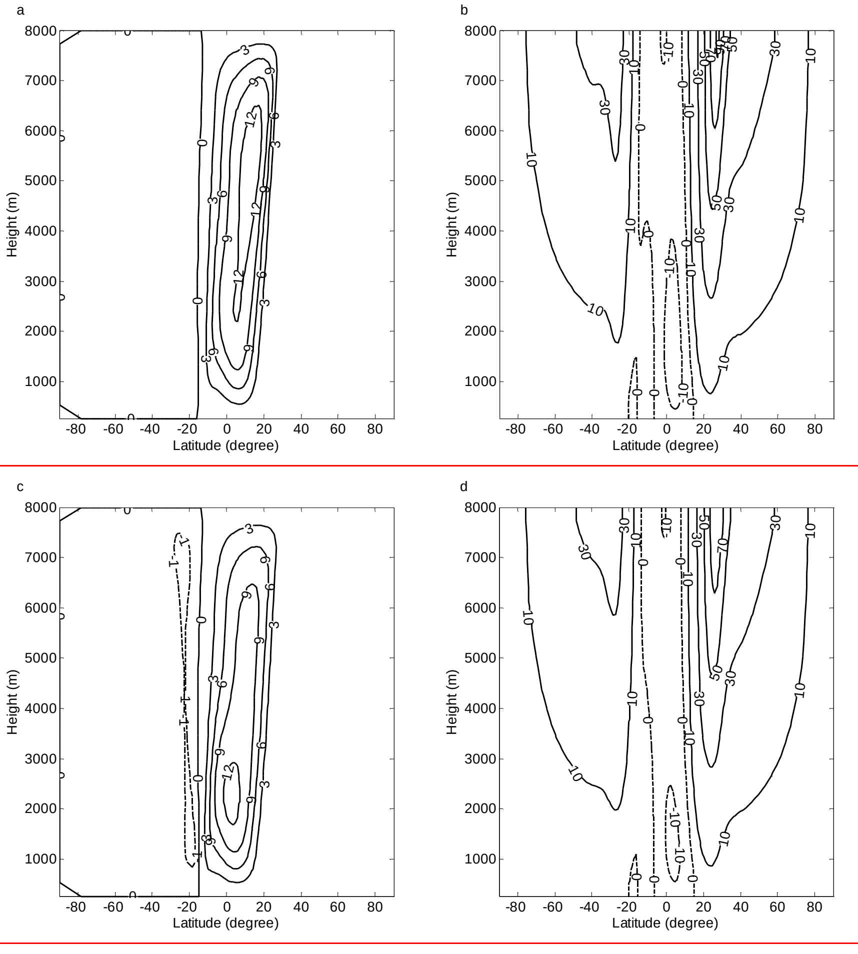
a
b
c
d
Height (m)
Latitude (degree)
8000
7000
6000
5000
4000
3000
2000
1000
-80 -60 -40 -20 0 20 40 60 80

~~Figure 12.~~

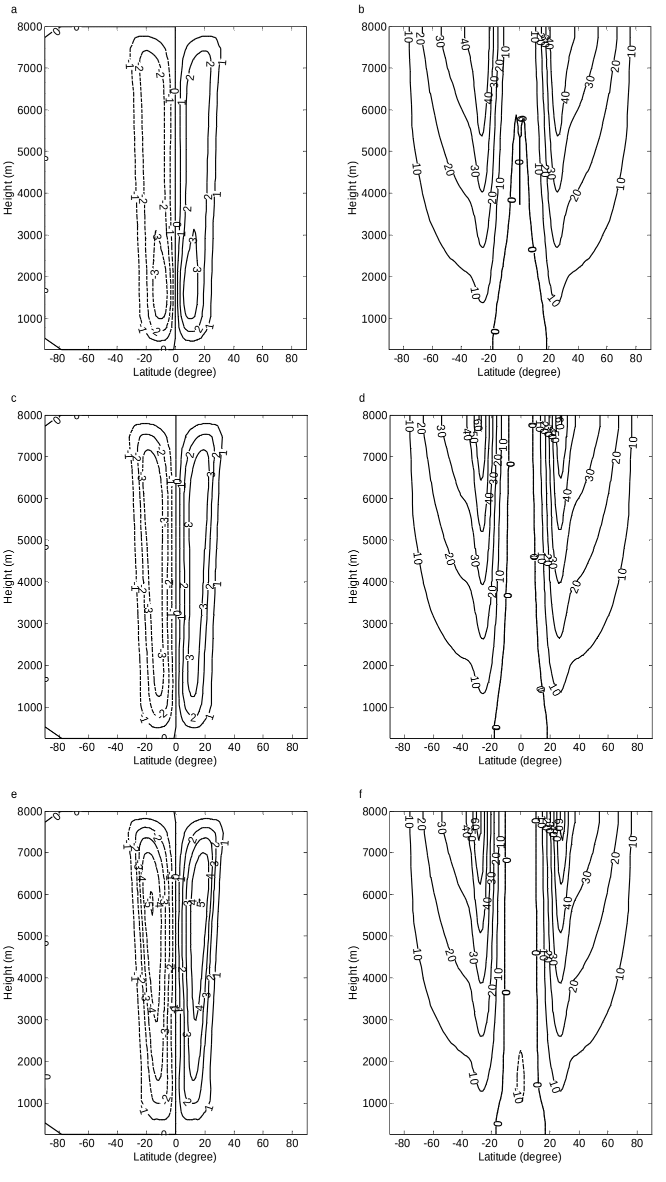

~~Figure 13.~~

Formattato

Formattato: Default Style

Pagina 1: [1] Definizione stile	Nazario	08/01/2015 08:51:00

Stile predefinito: Non regolare lo spazio tra testo asiatico e caratteri numerici, Allineamento carattere: Linea di base

Pagina 1: [2] Definizione stile	Nazario	08/01/2015 08:51:00

Soggetto commento: Non sillabare, Non regolare lo spazio tra testo asiatico e caratteri numerici, Allineamento carattere: Linea di base

Pagina 1: [3] Definizione stile	Nazario	08/01/2015 08:51:00

Testo commento: Non sillabare, Non regolare lo spazio tra testo asiatico e caratteri numerici, Allineamento carattere: Linea di base

Pagina 1: [4] Definizione stile	Nazario	08/01/2015 08:51:00

Collegamento ipertestuale: Colore carattere: Blu

Pagina 1: [5] Definizione stile	Nazario	08/01/2015 08:51:00

Normale (Web): Non sillabare, Non regolare lo spazio tra testo asiatico e caratteri numerici, Allineamento carattere: Linea di base

Pagina 1: [6] Definizione stile	Nazario	08/01/2015 08:51:00

Testo fumetto: Non regolare lo spazio tra testo asiatico e caratteri numerici, Allineamento carattere: Linea di base

Pagina 1: [7] Definizione stile	Nazario	08/01/2015 08:51:00

Intestazione: Non regolare lo spazio tra testo asiatico e caratteri numerici, Allineamento carattere: Linea di base

Pagina 1: [8] Definizione stile	Nazario	08/01/2015 08:51:00

Frame Contents: Non regolare lo spazio tra testo asiatico e caratteri numerici, Allineamento carattere: Linea di base

Pagina 1: [9] Definizione stile	Nazario	08/01/2015 08:51:00

Table Heading: Non regolare lo spazio tra testo asiatico e caratteri numerici, Allineamento carattere: Linea di base

Pagina 1: [10] Definizione stile	Nazario	08/01/2015 08:51:00

Table Contents: Non regolare lo spazio tra testo asiatico e caratteri numerici, Allineamento carattere: Linea di base

Pagina 1: [11] Definizione stile	Nazario	08/01/2015 08:51:00

Sottotitolo: Non regolare lo spazio tra testo asiatico e caratteri numerici, Allineamento carattere: Linea di base

Pagina 1: [12] Definizione stile	Nazario	08/01/2015 08:51:00

Piè di pagina: Non regolare lo spazio tra testo asiatico e caratteri numerici, Allineamento carattere: Linea di base

Pagina 1: [13] Definizione stile	Nazario	08/01/2015 08:51:00

Index: Non regolare lo spazio tra testo asiatico e caratteri numerici, Allineamento carattere: Linea di base

Pagina 1: [14] Definizione stile	Nazario	08/01/2015 08:51:00

Didascalia: Non regolare lo spazio tra testo asiatico e caratteri numerici, Allineamento carattere: Linea di base

Pagina 1: [15] Definizione stile	Nazario	08/01/2015 08:51:00

Elenco: Non regolare lo spazio tra testo asiatico e caratteri numerici, Allineamento carattere: Linea di base

Pagina 1: [16] Definizione stile	Nazario	08/01/2015 08:51:00

Text Body: Non regolare lo spazio tra testo asiatico e caratteri numerici, Allineamento carattere: Linea di base

Pagina 1: [17] Definizione stile	Nazario	08/01/2015 08:51:00

Heading: Non regolare lo spazio tra testo asiatico e caratteri numerici, Allineamento carattere: Linea di base

Pagina 1: [18] Definizione stile	Nazario	08/01/2015 08:51:00

Default Style: Non regolare lo spazio tra testo asiatico e caratteri numerici, Allineamento carattere: Linea di base

Pagina 1: [19] Definizione stile	Nazario	08/01/2015 08:51:00

Car. predefinito paragrafo

Pagina 1: [20] Definizione stile	Nazario	08/01/2015 08:51:00

Titolo 9: Non regolare lo spazio tra testo asiatico e caratteri numerici, Allineamento carattere: Linea di base

Pagina 1: [21] Definizione stile	Nazario	08/01/2015 08:51:00

Titolo 8: Non regolare lo spazio tra testo asiatico e caratteri numerici, Allineamento carattere: Linea di base

Pagina 1: [22] Definizione stile	Nazario	08/01/2015 08:51:00

Titolo 7: Non regolare lo spazio tra testo asiatico e caratteri numerici, Allineamento carattere: Linea di base

Pagina 1: [23] Definizione stile	Nazario	08/01/2015 08:51:00

Titolo 6: Non regolare lo spazio tra testo asiatico e caratteri numerici, Allineamento carattere: Linea di base

Pagina 1: [24] Definizione stile	Nazario	08/01/2015 08:51:00

Titolo 5: Non regolare lo spazio tra testo asiatico e caratteri numerici, Allineamento carattere: Linea di base

Pagina 1: [25] Formattato	Nazario	08/01/2015 08:51:00

Tipo di carattere: Non Corsivo